Cancer-Stem-Cell-Like, Wnt/TCF Responsive Cells Are Activated by Pax8 PPARγ Fusion Protein

by

Dang L. Vu-Phan

A dissertation submitted in partial fulfillment

of the requirements for the degree of

Doctor of Philosophy

(Cellular and Molecular Biology)

in The University of Michigan

2013

Doctoral Committee:

Professor Ronald J. Koenig, Co-Chair

Professor Max S. Wicha, Co-Chair

Professor Mark L. Day

Assistant Professor Ivan Patrick Maillard

Professor Richard M. Mortensen

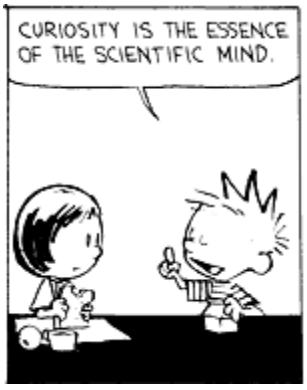

...

- Bill Watterson, 23 Apr 1993

DEDICATION

To my Parents and my family

who made sure I was brought up

safe and secure and never inhibited from indulging my curiosity.

To Oanh, my partner in all things

In memory of cô Triệu, who always made sure my thesis was going well.

I wish you were here.

TABLE OF CONTENTS

DEDICATION ii

LIST OF FIGURES iv

LIST OF TABLES v

ABSTRACT vi

CHAPTER

1. Introduction 1
2. Cancer-Stem-Cell-Like, Wnt/TCF Responsive Cells Are Activated by Pax8 PPARγ Fusion Protein 16
3. Establishing cell lines and an immune competent syngeneic tumor initiation model from PPFP/PTEN$^{thy-/-}$ mice. 46
4. PPFP expression increased ALDH activity and sphere formation 56
5. Akt activation did not mediate TCF/Wnt activation in PPFP cells 64
6. Discussion 70

BIBLIOGRAPHY 77

LIST OF FIGURES

Figure 2.1 Expression of PPFP in stably transfected PCCL3 cells. 36
Figure 2.2 Increased TCF driven GFP expression in PCCL3-PPFP cells. 38
Figure 2.3 Increased Soft agar colony formation in TCF_GFP+ cells. 39
Figure 2.4 Increased TCF activation after pioglitazone treatment. 40
Figure 2.5 SR1664 does not inhibit thyroid tumor growth in vivo. 42
Figure 3.1 PPFP/PTENthy-/- cells in dissociated mouse thyroid tumors. 50
Figure 3.2. Cells from dissociated PPFP+/PTEN-/- tumors growing on Matrigel coated plates. 52
Figure 3.3. TCF activation in PPFP/PTEN-/- cells. 53
Figure 3.4. H&E stained sections of spontaneous tumors from PPFP+/PTENthy-/- mice. 54
Figure 4.1. ALDH staining of typical tissue microarray samples. 60
Figure 4.2. ALDH activity in a minority of human FTC cells. 61
Figure 4.3. Increased ALDH1A1 with PPFP expression. 62
Figure 4.4. Increased sphere formation by PPFP cells. 63
Figure 5.1. Increased Akt activation in PPFP cells. 67
Figure 5.2. Non-concurrent activation of Akt and TCF. 68
Figure 5.3. Increased TCF activation after GSK3β inhibition. 69

LIST OF TABLES

Table 2.1. Genes in common between the expression profiles of PPFP thyroid carcinomas identified by Lacroix et al. (105) and Giordano et al. (24). 43
Table 2.2. Connectivity Map results showing the congruence of the common PPFP profile and gene expression changes caused by pioglitazone treatment. 44
Table 2.3. Small molecules which elicited similar gene expression changes to the common PPFP profile, which were also Chembank HTS standard hits for Wnt inhibitor, Wnt/Lithium modulators, or β-catenin inducer/translocator. 45
Table 3.1. Summary of tumor forming efficiency. 55

ABSTRACT

Pax8 PPARγ Fusion Protein (PPFP) occurs in ~35% of follicular thyroid carcinoma cases. Expression of PPFP in the non-transformed rat thyroid cell line PCCL3 conferred on the cells the ability to invade through matrigel and to form colonies in anchorage independent conditions.

PPFP also increased the percentage of cells that have activated β-catenin/TCF. We transduced control and PPFP-expressing PCCL3 thyroid cell lines with two different β-catenin/TCF-GFP reporter systems. PPFP expressing cell lines contained more than twice the percent of GFP positive cells compared to control cell lines.

A hierarchy existed within the cell lines based on the TCF activation status. A single TCF_GFP+ cell generated a clonal population containing both GFP+ and GFP- cells, whereas clonal populations derived TCF_GFP- cells remained GFP-. Single cells sorted by TCF status demonstrated that very few TCF_GFP- cells can generate any TCF_GFP+ cells.

The TCF responsive cells exhibited increased proliferative potential and invasive

capacity. GFP+ cells were twice as enriched for anchorage independent colony forming cells than GFP cells. More strikingly, GFP positive clones were 5-10 times more invasive than negative clones, which exhibited the same invasive potential as control cells.

The hierarchy and more transformed phenotype of TCF responsive cells indicate that they have the in vitro properties of cancer stem cells.

Full agonists of PPARγ further increased the effects of PPFP. The β-catenin/TCF population in PPFP expressing cells increased again while similarly treated empty vector control cells were unaffected. Invasion was also increased by the PPARγ agonists. The effects were blocked by PPARγ antagonists, demonstrating PPARγ specificity. Selective PPARγ agonists which only activate a fraction of the PPARγ effects also increased the effects of PPFP. We could then assume that the adipogenic pathways activated by full agonists but not selective PPARγ agonists did not contribute to PPFP oncogenesis.

These data suggested that PPFP acts via its PPARγ domains to expand the Wnt/TCF active cell fraction and that these cells have the properties of cancer stem cells. The pathways by which PPFP effect oncogenesis are activated by both full and partial PPARγ agonists.

CHAPTER 1

INTRODUCTION

Thyroid carcinomas are the most common cancers in the endocrine system. While the majority of cases are well-managed, significant mordibity and mortality occur when tumors recur or metastasize and are resistant to surgery and radioiodine, as there are no effective cytotoxic therapies. Potential new treatment options for these cases include targeted therapies against specific pathways that affect tumor growth or cancer stem cells (CSC), the hypothesized self-renewing source of malignant disease.

Our studies focused on a common chromosomal rearrangement found in follicular thyroid cancer (FTC). The paired box 8 (PAX8) - peroxisome proliferator-activated receptor γ (PPARγ) fusion protein (PPFP) resulting from the rearrangement imparted a more transformed phenotype when expressed in a non malignant thyroid cell line. The effects of PPFP were mediated by its PPARγ domains and effecting an enlarged subpopulation of cells with β-catenin/TCF activity and CSC-like properties. Our studies suggest that TCF reporters could be used to identify other thyroid CSCs and that PPARγ modulators could be potent clinical reagents against PPFP driven cancers.

Thyroid Gland

The thyroid gland is an endocrine organ whose secretions - thyroid hormones - control basal metabolic and biosynthetic rates. It consists of two elongated lobes connected by a central isthmus. The thyroid is wrapped against the front of the trachea, with the central isthmus on the midline and the lobes to the side.

The thyroid is composed of spherical subunits called follicles that are essential to the gland's hormone producing function. Each follicle is composed of a layer of epithelial cells - called thyroid follicular cells or thyrocytes - surrounding a protein rich colloid. Thyrocytes synthesize thyroglobulin (Tg) and concentrate Iodine ions into the colloid. Thyrocytes also synthesize thyroid hormones from iodinated Tg from the colloid and release them into the surrounding vasculature.

Thyrocytes which make up the basic functional subunit of the thyroid gland are mainly regulated by thyrotropin / thyroid stimulating hormone (TSH). TSH stimulation commits multipotent cells to a thyroid differentiation program (1–3). In the mature thyroid, TSH regulates the expression levels of many thyroid genes including Tg, Sodium/Iodine symporter (NIS), and Paired box 8 (Pax8) (4–7). TSH also regulates the proliferation of thyrocytes themselves, in the process modulating many fundamental cellular (and oncogenic) pathways (8). Conversely TSH production in the pituitary is inhibited by thyroid hormone (TH) while Tg levels affect thyrocyte gene expressions themselves (9;

10).

The profound effects of TSH on thyrocytes are the basis of its physiological and clinical roles. TSH was first identified as a secreted factor which controls thyroid function (11). Serum levels of thyroid hormones are regulated by TSH secretion. Overproduction of TSH due to pituitary tumors or inappropriate activation of the TSH receptor (TSHR) by auto-antibodies (Graves' disease) are causes of hyperthyroidism, while low TSH production due to hypopituitarism or insufficient response to TSH are causes of hypothyroidism. Recombinant or synthetic TSH is used clinically to stimulate radioiodide uptake in thyroid neoplastic disorders, and synthetic TH, one of the most commonly prescribed drugs in the United States, is used to treat TH deficiency.

Of course, TSH is not the only factor controlling thyrocyte biology. Insulin and Insulin-like growth factor (IGF) are well-characterized enhancers of the mitogenic effects of TSH (12; 13). Depending on the culture system, thyrocyte proliferation is also stimulated by basic fibroblast growth factor (bFGF), epidermal growth factor (EGF), and hepatocyte growth factor (HGF). bFGF and EGF are also important for the maintenance and growth of putative thyroid stem cells (14; 15). Unsurprisingly, TSH and the growth factors also have important roles in thyroid carcinomas.

Thyroid Carcinoma

Thyroid carcinomas occur when thyrocytes proliferate uncontrollably and spread beyond

their physiological confines. Standard therapies - surgery, radioactive iodine, and TSH suppression - for thyroid carcinomas are often effective. Nonetheless, 1780 deaths are estimated to result from thyroid carcinomas this year from metastatic and therapy resistant disease (16; 17). For these cases, new therapies are needed, targeting the specific biological processes and genetic alterations that drive tumor growth.

Thyroid carcinomas are often first detected as thyroid nodules, a sign of irregular growth in the thyroid gland. The vast majority of these nodules are benign growths. The first diagnsotic step is then to rule out obvious cases of hyperfunctioning thyroids. If thyroid function is normal, which is usually the case, the presence of a radiographically distinct nodule may be confirmed by ultrasound imaging. If confirmed, extractions of sample thyroid tissues with fine-needle aspirations (FNAs) are performed. Suspicious lymph nodes in the locality are also sampled. Diagnoses are attempted after histological examination of collected tissues (18).

Tissue architecture and cellular structure differences classify thyroid carcinomas into 3 basic histologic types. Differentiated thyroid carcinomas (DTC) are the most common and feature cells which retain many features of normal thyrocytes. Medullary thyroid carcinomas (MTC) arise not from follicular thyrocytes but parafollicular cells which normally produce calcitonin, not Tg. Anaplastic thyroid carcinomas (ATC) are completely undifferentiated, aggressive, therapy resistant, and usually fatal cancers. Nonetheless, differentiated thyroid carcinomas still account for most thyroid cancer-

related deaths since they constitute a vast majority of thyroid cancer cases (17; 18).

DTCs are classified by histological appearances. Papillary thyroid carcinomas account for more than 85% of DTCs. PTCs are etymologically derived from the replacement of traditional follicular structures by papillae - several layers of neoplastic thyroid epithelial cells lining a fibrous core. Presently PTC are identified by certain characteristic nuclear features such as larger, clearer nuclei with inclusion bodies of cytoplasm and nuclear grooves (19). Follicular thyroid carcinomas (FTCs) account for most of the remaining DTC cases. Presently FTCs are identified both by follicular structures and by the lack of PTC nuclear features. The differences between FTCs and PTCs are not always clear, and there are suggestions that some follicular variant PTCs are biologically more similar to FTCs (20). Diagnoses of FTCs also depend on evidence of invasion in the tissue sample, therefore the differences between FTCs and benign follicular adenomas (FA) are also not always apparent (18; 20).

Distinct molecular changes are associated with each of the histology types. These provide valuable insights about the biology of each tumor types and suggest potential therapeutic strategies. They may also be useful as diagnostic tools but the data are not yet robust enough for these molecular markers to be recommended for routine use (18).

Surgery - either partial or total thyroidectomy is the primary treatment option for thyroid carcinomas. Regional lymph nodes which harbor metastases should also be excised. For

organ confined tumors or those that have only invaded locally, surgery can be curative and 5 year survival is higher than 97% (16; 18).

Treatments which take advantage of the specific biology of thyrocytes are used to prevent recurrence or to treat residual disease or recurrrent metastatic disease. Because thyrocytes concentrate Iodine, radioactive iodine can be used to identify as well as ablate remnant thyroid carcinoma tissues that retain that particular function. Stimulation with recombinant TSH and/or TH withdrawal are also used to boost radioiodine uptake. Treatment with levothyroxine, a synthetic thyroid hormone, is aimed at lowering the serum level of TSH and preventing recurrence (17; 18).

There are few durable treatments for metastatic disease which does not concentrate iodine. About 20-25% of FTC and 10% of PTC patients develop distant metastases. Survival for these patients (35% at 5 years) is much lower than for those with locally limited disease (>97%). The lungs are the most common site of metastasis (50-65%), followed by the skeleton (20%) and central nervous system. External-beam radiation therapy may be used palliatively to reduce tumor burden, but is rarely curative. Studies show that the response rate to cytotoxic chemotherapy such as doxorubicin is only 2-25% (17; 18; 21).

Targeted Therapies

The development of more effective treatments for refractory disease depend on deeper

understanding of biological processes that underlie oncogenesis. As mentioned earlier, histologically distinct classes of thyroid cancer are associated with distinct mutations. PTCs often include the Ret/PTC translocation, activating BRAF mutations, or activating Ras mutations (mostly in follicular variant PTC). Ras mutations and the Pax8/PPARγ translocation are found in more than 75% of FTCs. These mutations are generally mutually exclusive and tumors harboring each mutation have characteristic transcriptional programs (22–26). It is hoped that compounds which target these seemingly fundamental mutations and other dysregulated pathways would be efficacious while having fewer side effects than cytotoxic chemotherapy.

The development of drugs targeting driving mutations have led to significant improvements in therapy of other cancer types. For example, Imatinib (Gleevec) is famously the "magic bullet" against chronic meyologenous leukemia harboring the Bcr/Abl translocation (27; 28). Trastuzumab (Herceptin) increases survival and reduces recurrence in Her2 amplified breast cancer (29–31). Erlotinib (Tarceva) and gefitinib (Iressa) achieved tumor response and increased progression free survival in non small cell lung cancer harboring activating EGFR mutations (32; 33).

A number of pre-clinical studies and clinical trials have been conducted to develop similarly targeted drugs against thyroid cancer (34). Vandetanib (Caprelsa) a tyrosine kinase inhibitor effective against RET, VEGFR, and EGFR is the first drug approved for MTC (35). Data suggest it may also be effective against differentiated thyroid cancers

(36). Another tyrosine kinase inhibitor effective against RET and Met - XL184 (Cabozantinib) is seeking FDA approval for treating MTC after successful clinical trials (37; 38). Our lab is proceeding with our pre-clinical data showing excellent and surprising efficacy of the drug Pioglitazone against a transgenic mouse model of PPFP expressing thyroid cancer (39).

Another important source for identification of novel targets for the treatment of thyroid cancer is emerging from an understanding of cancer stem cell biology. CSCs are hypothesized to be therapy resistant, slowly cycling cells which can repopulate decimated tumors following treatment or initiate new metastatic tumors in distant sites . The presence of CSCs within the previously thought to be flat tumor hierarchy has important clinical implications: resistance arises not from selection of increasingly resistant cells from a stochastically variable population but from intrinsically resistant CSCs that give rise to proliferative progeny. Traditional drugs developed for their ability to shrink tumors fail because they neglect the small number of regenerative CSCs that remain after cytotoxic chemotherapy. Supporting this and echoing findings in other tissues, remnants of ATC treated with doxorubicin were found to be almost entirely composed of CSC-like cells (40).

Thyroid Cancer Stem Cells

The existence of cancer stem cells is an old concept made testable by recent advances in cell sorting technology and xenotransplantation assays. The inefficiency with which

cancer cells form new tumors was established long ago. It has been hypothesized to be due either to a random spread of phenotypic variability and procedural attrition or to a limited sub population of cells that could initiate tumors. Fluorescence-activated cell sorting (FACS) segregates cells based on intrinsic characteristics and defines sub-populations with vastly different tumor forming capacity in immune-compromised or syngeneic mice, in support of the latter hypothesis (41).

In addition to tumor initiating capacity, a number of other properties have been described in CSCs. A clonal population derived from CSCs is predicted to be multipotential and capable of regenerating the heterogeneity of the original tumor. If distant metastases are initiated by CSCs, invasiveness must be a characteristic of at least some CSCs. The multiple metastases and recurrences require that CSCs, like stem cells, have extensive self-renewal capacity. As previously stated, CSCs are also resistant to conventional cytotoxic therapy, remaining behind to reconstitute apparently eradicated tumors.

A number of strategies have been attempted to isolate thyroid CSCs:

Side population (SP) cells are cells which do not retain the fluorescent Hoechst DNA binding dye due to their high levels of transporter proteins. SP cells are present in mouse thyroid, human goiters (a source of proliferating but non-malignant thyroid cells), and thyroid cancer cell lines. These cells express stem cell genes and have higher colony forming efficiency, a measure of high proliferative capacity, if not self-renewal (15; 42;

43). SP thyroid cancer cells are also chemotherapy resistant and have enhanced but not exclusive tumor-initiating capability (40; 43).

A subset of thyroid cancer cells express CD133, a cell surface protein recognizable by well-characterized antibodies. CD133+ cells are reported in ATC and MTC primary samples and ATC cell lines. CD133+ cells express stem cell genes and exhibit increased self-renewal (44; 45). CD133+ ATC cells are reported to display chemotherapy resistance, exhibit epithelial to mesenchymal transition (EMT) markers associated with invasiveness, and are exclusively able to generate tumors in immune compromised mice (44; 46; 47). Targeting stem cell associated pathways reduce the number and chemotherapy resistance of CD133+ ATC cells (48).

Aldehyde dehyrogenase (ALDH) is a detoxifying and differentiation signal transducing enzyme elevated in stem cells (49; 50). A fluorescent assay marking cells with ALDH activity can be used to isolate normal and malignant stem cells from a variety of tissues (51–53). Cells exhibiting high ALDH activity are found in all types of thyroid cancer, with lower percentages in differentiated types and the highest percentage in undifferentiated, aggressive thyroid cancers. $ALDH^{high}$ cells form more colonies or "spheres" in serum-free, suspension cultures and generate heterogenous tumors when injected subcutaneously or into the thyroid while $ALDH^{low}$ cells do not (54).

Cells with stem cells like properties can also be collected without prior assumption of

surface markers or protein expression. Colony or sphere forming assays selectively enable the growth of stem and progenitor cells while more differentiated cells die off. In the thyroid, suspension cultures collected multipotential cells that do not express thyroid-specific markers but can be induced to re-express them (15; 55). Drugs which inhibit CSCs - such as Metformin, which sensitized ATC to doxorubicin treatment via a CSC-dependent mechanism - also tended to inhibit colony formation in suspension cultures (56).

Studies of CSC populations reveal a number of insights into their biology and suggest new therapeutic targets. Both CD133+ and $ALDH^{high}$ cell fractions are significantly increased by TSH stimulation (47; 54), which could be one reason why TSH suppression therapy is oftentimes successful in thyroid cancer. Culture conditions of colony or sphere forming assays suggest that CSCs depend on EGF and bFGF for self-renewal. Gene expression analysis of the spheres show differential expression of insulin receptors and insulin-like growth factor receptors on thyroid cancer stem cells compared to normal thyroid stem cells (57). The Ret proto-oncogene has been suggested to play a role in regulation of PTC and MTC stem cells (45; 58) while constitutive activation of c-Met and Akt pathways are implicated in undifferentiated thyroid cancers (54).

Another as yet unexplored way to identify thyroid cancer stem cells is to transfect a reporter gene into a population such that cells with a certain pathway activated express an identifying protein. This strategy, applied to the Wnt/β-catenin/TCF pathway, is

spectacularly successful in intestinal, colorectal, and other tissues.

Wnt/β-catenin/TCF pathway

The Wnt/β-catenin/TCF pathway is a central pathway in developmental, cancer, and stem cell biology. The pathway is activated by the binding of a Wnt ligand to a cell surface receptor. Signal transduction within the cells eventually leads to stabilization, activation, and nuclear translocation of β-catenin. TCF, β-catenin and other proteins form a transcription complex activating the multitude of genes in the Wnt/β-catenin/TCF program. Mutations or dysregulation of the pathway leads to developmental defects and cancers. β-catenin/TCF activity regulates self-renewal and is recognized as the distinguishing feature of normal and cancer stem cells in many tissues (59).

Wnt/β-catenin/TCF dysregulation is common in ATC and there is evidence that it occurs in differentiated thyroid cancers as well. Gain of function mutations of β-catenin are present in about half of ATC cases, leading to high levels of β-catenin nuclear translocation (60; 61). Loss of function mutations of the Wnt signalling inhibitor Axin are found in 80% of ATC (62) while a germline mutation of a different Wnt inhibitor APC leads to PTC (63; 64). Aberrant cytoplasmic localization of β-catenin is common in FTC and PTC, but there is little evidence that β-catenin is also present at the nucleus (65; 66). Nonetheless, overexpression of Wnt target genes Myc and Cyclin D1 often correlates with theaberrant β-catenin localization (65; 66).

Many signalling pathways known to be dysregulated in thyroid cancers also affect β-catenin/TCF transcriptional activity. Akt, aberrantly activated in ATC as well as our transgenic model of PPFP expressing thyroid carcinoma, is a well known inhibitor of GSK3-β, a β-catenin inhibitor. Akt also directly activates β-catenin through phosphorylation (67). Proteins which affect β-catenin via Akt include the previously mentioned c-Met and RET as well as PTEN, whose mutation leads to Cowden syndrome and thyroid cancer (68–73). Sulindac, a non-steroidal anti-inflammatory drug reverses the nuclear translocation of β-catenin in a BRAFV600E dependent manner in PTC, suggesting that BRAF can regulate β-catenin as well (74).

In other tissues, the Wnt/β-catenin/TCF pathway is well known as the central regulating pathway of normal and malignant intestinal and colorectal stem cells. Colon cancer is the significantly more common cancerous manifestation of germline APC mutations (75). A reporter assay first identified constitutive activation of β-catenin/TCF transcription as the key consequence of APC loss of function leading to malignant transformation (76). TCF4 (TCF7L2) is required for maintenance of the intestinal stem cell compartment (77) and expression of Lgr5, a target of the Wnt/β-catenin/TCF pathway, identifies normal and cancer intestinal and colorectal stem cells (78–81). TCF reporter activity also identifies tumor forming colorectal CSCs (82).

TCF activity assays indicate that there is activation of the Wnt/β-catenin/TCF pathway in thyroid cancer, as is expected from the many pathway-related mutations discussed above.

Wnt/β-catenin/TCF responsiveness is found in the ARO ATC cell line, RET/PTC1 cell line model of PTC, and a mutant thyroid hormone receptor model of thyroid cancer (83–85). TCF responsive elements drive the expression of luciferase in these experiments and the results indicate the population-wide average level of TCF activity without providing information about heterogeneity within the population. Nonetheless, TCF activity may be a marker of thyroid CSCs as as is the case in other tissues.

Conclusion

New treatment options are needed for thyroid cancers resistant to conventional therapy. Two promising avenues of research are targeted therapies against known genetic alterations and against cancer stem cells. The two strategies are not mutually exclusive. Many of the genetic alterations that confer survival advantages to the bulk tumoralso play a role in regulating CSCs. Drugs targeting CSCs specifically are still going through the clinical trial process but the surprising effectiveness of Trastuzumab even on HER2 negative breast cancer can be traced to its effects on previously unrecognized HER2 pathways in breast CSCs (86).

The Wnt/β-catenin/TCF pathway is a well characterized stem cell pathway that is thought to be downstream of many of the altered pathways in thyroid carcinoma. Our data provide the first evidence that TCF responsiveness is a possible marker of thyroid cancer stem cells and link the expansion of the CSC-like TCF responsive fraction to the activity of the PPARγ domains of PPFP. PPARγ is a much studied clinical target and the ability to

influence thyroid CSCs via PPARγ modulators suggests exciting new directions for research.

CHAPTER 2

Cancer-Stem-Cell-Like, Wnt/TCF Responsive Cells Are Activated by Pax8 PPARγ Fusion Protein

INTRODUCTION

The paired box 8 (PAX8) - peroxisome proliferator-activated receptor gamma (PPARγ) fusion protein (PPFP) results from a genetic lesion implicated in the etiology of ~35% of follicular thyroid carcinomas (FTCs) (87). A t(2;3)(q13;p25) chromosomal translocation fuses the promoter and most of the *PAX8* structural gene to the coding exons of the *PPARG* gene. Since the *PAX8* promoter is highly active in the thyroid, PPFP is expressed at a high level in thyroid carcinomas containing this translocation. Expression of PPFP increases cell growth, viability, and anchorage-independence in thyroid and non-thyroid cell lines (88–90).

Both fusion partners of PPFP play important roles in tissue development and differentiation. PAX8 is a transcription factor required for thyroid development and mature thyroid gene expression (91–96). PPARγ is a nuclear hormone receptor that has been well studied as the master regulator of adipocyte differentiation and as an important

therapeutic target for diabetes, atherosclerosis, inflammation and cancer (97). Modulation of PPARγ-regulated pathways is thought to be important in PPFP carcinogenesis, and this is consistent with the observation that a different translocation fusing *PPARG* to the gene *CREB3L2* also has occasionally been identified in FTC (98).

The initial report of PPFP occurrence and subsequent publications demonstrate that PPFP interferes with PPARγ transactivation in a dominant negative manner (87; 88). PPFP also can inhibit PPARγ action in experimental systems unrelated to FTCs (99; 100). The hypothesis that PPFP exerts its pro-oncogenic effect via repression of PPARγ is bolstered by observations that PPARγ is downregulated in other types of thyroid carcinoma, that restoration of PPARγ activity has therapeutic anti-proliferative, pro-differentiation effects, and that heterozygous deletion of *Pparg* enhances tumorigenesis in an unrelated mouse model of thyroid carcinoma (101–104).

Nonetheless, there is evidence that PPFP also can transactivate some PPARγ target genes. Numerous PPARγ target genes are upregulated in PPFP tumor samples versus non-PPFP FTC or normal thyroid (24; 105). I*n vitro*, PPFP stimulates the promoters of some PPARγ target genes, represses others, or both depending on the cellular context (24; 88; 89).

Thyroid specific expression of PPFP combined with thyroid specific knockout of *Pten* in a transgenic mouse model generates spontaneous metastatic follicular thyroid carcinoma (39). In the thyroids of these mice, PPARγ target genes can be positively or negatively

regulated by PPFP. With pioglitazone treatment, however, adipocyte PPARγ target genes are broadly upregulated and thyrocytes adopt an adipocyte phenotype, indicating that the functional domains of PPFP retain their capacity to act in a strongly PPARγ-like manner. Thus, overall, the actions of PPFP that contribute to thyroid carcinogenesis are poorly understood.

In this study we show that expression of PPFP in the rat thyroid PCCL3 cell line induces properties of transformation, including increased anchorage-independent growth and invasiveness. Transformation requires a functional PPARγ DNA binding domain (DBD) within PPFP and is further enhanced by PPARγ agonists. Our data also show that a small fraction of PCCL3 cells are Wnt/TCF-responsive, the responsive fraction is expanded by PPFP expression, and that fraction has properties of cancer stem cells.

MATERIALS AND METHODS

Cell culture and Reagents

The PCCL3 differentiated rat thyroid cell line has been described (106). PCCL3 cells and their derivatives were cultured at 5% CO_2 in Coon's F-12 media with L-glutamine supplemented with 5% fetal bovine serum and antibiotic/antimycotic (Thermo Scientific, Waltham, MA, US), 1mIU/ml TSH, 10μg/ml insulin, 5μg/ml apo-transferrin, 10nm hydrocortisone (Sigma-Aldritch, St. Louis, MO, US) and prophylactic plasmocin (Invivogen, San Diego, CA, US).

SR1664 was a gift from Drs. Patrick Griffin and Bruce Spiegelman. GW9662 and T0070907 were purchased from Cayman Chemicals (Ann Arbor, MI, US). Bvt.13 was purchased from Sigma-Aldritch. Myc antibody was purchased from Cell Signaling Technology (Danvers, MA, US, catalog #2276) and GAPDH antibody sc-32233 was from Santa Cruz Biotechnology (Santa Cruz, CA, US).

Stable Transfection

The P box amino acids EGG within the PPARγ DBD of PPFP were mutated to AAA by inverse PCR to generate PPFP-AAA, and the entire sequence was verified. PPFP or PPFP-AAA with 3 Myc epitopes at the N terminus was inserted into the pCagen plasmid (Addgene, Cambridge, MA, US, plasmid 11160) (107). pCagen-PPFP, pCagen-PPFP-AAA or pCagen empty vector control plasmid was co-transfected at 10-fold excess with a hygromycin resistance vector (Clontech, Mountain View, CA, US, #631625) into PCCL3 cells using Fugene 6 (Promega, Fitchburg, WI, US). Transfected cells were then plated at clonogenic density and subjected to hygromycin B selection at 400 μg/ml. Resistant colonies were assayed for PPFP by RT-PCR and Western blot.

DNA Binding Assay

The DNA binding activities of PPFP and PPFP-AAA were assessed using an avidin biotin complex to DNA assay (108) with minor modifications. Whole cell lysates were generated from the appropriate stably transfected PCCL3 cells using M-PER (Thermo Scientific) supplemented with 0.4M NaCl and Halt Protease Inhibitor Cocktail (Thermo

Scientific). Fifty μg of lysate protein were incubated with a double stranded oligonucleotide, biotinylated at the 5' end of the top strand, that contains the mouse *Aqp7* gene PPAR response element. The top strand sequence is AGTTCTGTTGTGCTTCTCCAGGGGAGAGGTCAGTAGGGCAGGGGTTT, and the minimal response element is underlined. A mutated sequence was used as a specificity control in which the underlined sequence was changed to ATTTGAGATTTCA. Protein-DNA complexes were pulled down with NeutrAvidin agarose beads (Thermo Scientific), and were then subjected to electrophoresis through an SDS polyacrylamide gel and analyzed for PPFP by Western blot using a Myc antibody.

Lentiviral Construction and Infection

All lentivirus construction was done at the University of Michigan Vector Core. Lentiviral TOP-destabilized green fluorescent protein (dGFP) construct was a gift of Dr. Irving Weissman through Dr. Hasan Korkaya. pGreenFire TCF/LEF lentivirus reporter was obtained from System Biosciences (Mountain View, US). In this construct, dGFP expression is driven by a minimal CMV promoter preceded by four TCF/LEF response elements. The same pGreenFire reporter but lacking TCF binding sites was used as a control to set flow cytometry gates for GFP positivity. Cells were infected with 10X concentrated particles provided by the Core, supplemented with 5μg/ml polybrene. 5 days after infection, cells were checked for GFP expression. GFP positive cells were isolated via fluorescence activated cell sorting and replaced in culture to obtain 100% transduced cell lines.

Flow Cytometry

Flow cytometric analysis and sorting was done at the University of Michigan Flow Cytometry Core. Cells to be run on a flow cytometer were filtered through a 40 micron sieve after removal from culture. Cell were resuspended in Hank's Balanced Salt Solution (HBSS) with propidium idodie (PI) or 4′,6-diamidino-2-phenylindole (DAPI) added as a viability indicator. At least 10,000 live cell events were recorded during each run of a cell sample through the flow cytometer. Gates were set at the level of GFP expression in 99.5% of control cells expressing GFP under the control of the minimal CMV promoter without TCF response elements. Test samples with GFP levels higher than gated were considered GFP positive and TCF responsive.

Soft Agar Colony Formation Assay

Live trypsinized cells in 0.2% trypan blue were counted on a hemocytometer, where we also verified that at least 95% of cells were singlets. 5000 cells were resuspended in 333 µl full media, thoroughly mixed with 667 µl full media + 0.5% low melt agarose, and added to a well in a 24 well ultra low attachment plate. After the agarose set, 100µl of full media was added to cover the well. Additional media was added every 5 days to maintain coverage. After 21 days, cells were stained with 0.025% crystal violet and colonies counted under a microscope.

Matrigel Invasion Assay

Cell culture inserts for 24 well plates from BD Biosciences (Franklin Lakes, NJ, US) were used with standard 24 well tissue culture plates. 100 µl 12.5% Matrigel (BD Biosciences) in unsupplemented F-12 media was added to each insert to cover the base of the top chamber. Matrigel was allowed to set in a 37^{o} incubator for 60 minutes. 600 µl Coon's F-12 media supplemented with 10% FBS was added directly to the bottom well. 5000 or 25000 single cells obtained as above were resuspended in 200 µl unsupplemented F-12 media and added to the upper chamber. After 36 hours the experiment was stopped by addition of 32% paraformaldehyde to a final concentration of 1.5%. Afterwards the media were aspirated and a gentle swabbing removed the matrigel layer and any remaining media. Cells on the bottom of the inserts were stained in a solution of 0.025% crystal violet, washed and stored in distilled water, and counted under a microscope.

Quantitative rt-PCR

Cells removed from culture by trypsinization was placed directly in RealTime Lysis Buffer (Roche Applied Science, Basel, Switzerland) and DNA synthesized directly from lysate using Transcriptor Universal cDNA Master. Primer and probe sets for the respective genes were ordered from Universal Probe Library (Roche). Quantitative rt-PCR was done on a Lightcycler 480 using Sybr Green I Master. Analysis was done by the LightCycler software at High Sensitivity setting (Roche).

Quantitative PCR for PPFP expression after transfection: RNA was isolated using an RNeasy mini kit (Qiagen, Venlo, Netherlands). cDNA was synthesized using SuperScript III (Invitrogen, Carlsbad, CA, US). Real-time PCR was performed using an Applied

Biosystems (Foster City, CA, US) Step One Plus real-time PCR instrument and Power SYBR Green master mix. In general, the cDNA from 100 ng RNA was used in triplicate PCR. Primer sets for PPFP: forward CGGACAGGGCAGCTATGC and reverse TCTCTGTGTCAACCATGGTCATT; for PPARγ: forward AGGCGAGGGCGATCTTG and reverse CATGTCGTAGATGACAAATGGTGAT.

In vivo studies

All *in vivo* studies were approved by the University of Michigan Committee on the Use and Care of Animals. FVB/N mice with combined thyroid-specific expression of PPFP and thyroid-specific deletion of *Pten* develop follicular thyroid carcinoma that is responsive to pioglitazone (39). Beginning at 8 weeks of age and continuing for 14 days, we treated these mice with either a control diet, or pioglitazone in the chow at 200 parts per million, or SR1664 by IP injection at 30 mg/kg body weight every 12 hours. SR1664 at 20 mg/kg is strongly insulin-sensitizing (109). Thyroid size was measured by ultrasound at the start and end of the two week treatment period as described (39).

Statistical Analyses

Statistical differences for colony growth, invasion, TCF activation, and gene expression were determined using the Students *t*-test function on Open Office Calc. $p<0.05$ was considered significant.

RESULTS

The PPARγ DBD within PPFP is essential for the ability of PPFP to induce a transformed cell phenotype.

The PCCL3 rat thyroid cell line (106) was stably transfected to express Myc-tagged PPFP or Myc-tagged PPFP with a mutated, non-functional DBD, described in more detail below. Expression of PPFP at the RNA level was 21 ± 2.1 fold above endogenous PPARγ by RT-qPCR (n=3), which is within the range of 10-50 fold typically seen in PPFP expressing thyroid carcinomas (24).

To determine whether PPFP activities depend on retention of a functional PPARγ DBD, we mutated the P box amino acids EGG at the base of the first zinc finger to AAA, and stably expressed this mutant PPFP protein in PCCL3 cells. Henceforth, the protein will be denoted PPFP-AAA and the cell line PCCL3-AAA. The PPFP and PPFP-AAA proteins were expressed at similar levels in their respective cell lines [Fig. 1A]. As expected given that P box amino acids contact the bases in the DNA response element (110), the AAA mutation prevented binding to a PPAR response element [Fig. 1B].

Compared to PCCL3 cells stably transfected with empty vector (PCCL3-EV), PCCL3-PPFP cells exhibited a more transformed phenotype. Thus, PCCL3-PPFP cells generated 8 times more colonies in soft agar [Fig. 1C] and 3 times as many PCCL3-PPFP cells invaded through Matrigel-coated transwells [Fig. 1D]. PCCL3-AAA cells did not exhibit increased colony formation or invasion [Fig. 1C, 1D], indicating that the PPARγ DBD within PPFP is important for these activities.

PPFP target genes overlap those from agonist induced PPARγ activation

Gene expression profiles of human PPFP thyroid carcinomas have been reported by Lacroix et al. and Giordano et al. (24; 105). Giordano identified 55 genes that were highly over-expressed specifically in PPFP carcinomas, and 17 of those 55 also were found by Lacroix to be over-expressed in PPFP tumors versus normal thyroids [Table 1]. We tested the expression of 5 of the 17 intersection genes by RT-qPCR and found that 3 of the 5 are induced in PCCL3-PPFP cells versus PCCL3-EV cells. The results for these 3 genes, Angiopoietin like 4 (ANGPTL4), Fibroblast Growth Factor Binding Protein 1 (FGFBP1), and Myelocytomatosis Viral Oncogene Homolog 1 (MYCL1), are shown in Fig. 1E. The expression of the other 2 genes, C-X-C chemokine receptor type 7 (CXCR7) and Tumor necrosis factor receptor superfamily member 21 (TFNRSF21), was not significantly changed (data not shown). These data indicate that the transcriptional effects of PPFP expression in this rat thyroid cell line overlap with the changes seen in human PPFP carcinomas.

We conducted a search on Connectivity Map (CMAP) (111) to identify bioactive small molecules that induce a set of gene expression changes similar to the set common to the Lacroix and Giordano PPFP profiles. The PPARγ agonist pioglitazone was among the top results returned ($p=0.014$ overall, $p=0.006$ for human prostate PC3 cells) [Table 2]. Other thiazolidinediones - rosiglitazone and troglitazone - also elicited significantly similar responses in PC3 cells ($p<0.05$) but their overall rankings in CMAP were diminished by

large variance in the MCF7 cell responses (data not shown). Both the Giordano and Lacroix gene expression profiles and their intersection include known PPARγ target genes, which provides countervailing data to the hypothesis that PPFP acts uniformly as a dominant negative suppressor of PPARγ.

PPFP is a potential modulator of the Wnt pathway.

Another emergent theme from the CMAP results was Wnt pathway modulation. Among the 70 bioactive small molecules significantly enriched for PPFP profile genes, 16 were standard hits in Chembank high-throughput screens (HTS) for Wnt inhibitors, Wnt/Lithium modulators, or β-catenin inducers/translocators [Table 3]. Of the 16, simvastatin, azacytidine, methotrexate, amiloride and anisomycin were also reported to impact on the Wnt pathway elsewhere in the literature (112–119).

Based upon this, we delivered via lentivirus two independent Wnt/TCF responsive promoter constructs driving GFP expression into our cell lines to measure the extent of Wnt pathway activation. GFP positive cells were sorted and grown to generate new cell lines in which all of the cells were transduced. With either construct and 3 independent PPFP cell lines we found a 2-5 fold increase in the number of TCF_GFP+ cells relative to similarly-infected PCCL3-EV control cells. As was the case with the functional assays, the DBD mutant PPFP-AAA did not effect an increase in TCF_GFP activation over control cells [Fig. 2A, 2B].

An apparent hierarchy exists in the cell lines defined by TCF activation status.

We sorted the 100% transduced cell lines into TCF_GFP+ and TCF_GFP- fractions. The TCF_GFP+ fraction again generated both TCF_GFP+ and TCF_GFP- populations. The TCF_GFP- fraction also regenerated TCF_GFP+ cells, but at a small fraction of the original level [Fig. 2C-E]. The TCF_GFP- fraction could have had a diminished but extant capacity to generate TCF_GFP+ cells, or the TCF_GFP+ cells could have come from contaminating, originally TCF_GFP+ cells. Clonal populations grown from single cells sorted into 96 well plates provided a more informative test which supports the latter possibility. Out of 26 EV control clones and 23 PPFP clones grown from TCF_GFP- cells, only one contained a significant TCF_GFP+ fraction, which was still a small fraction of the TCF_GFP+ fraction of the parental cell line [Fig. 2F]. The ability to reconstitute the heterogeneity of the parental cell lines was clearly confined to the TCF_GFP+ populations of the EV control and PPFP cell lines.

The TCF responsive cell fraction is enriched for anchorage independent and invasive cells.

Bulk populations of TCF_GFP+ cells formed more colonies in soft agar than TCF_GFP- cells [Fig. 3A]. Clones derived from TCF_GFP+ cells also formed more colonies than clones of TCF_GFP- cells, though overlap was observed [Fig. 3B]. Furthermore, clones of TCF_GFP+ cells were on average 5 times more invasive than clones of TCF_GFP- cells [Fig. 3C].

TCF activation in PCCL3-PPFP cells involves a cell autonomous process.

The signaling cascade leading to TCF activation typically originates from exogenous Wnt ligands, but exogenous factors were not sufficient to account for TCF activation in PCCL3-PPFP cells. PCCL3-EV control cells transduced with TCF_GFP were co-cultured with 4-fold excess PCCL3-EV or PCCL3-PPFP cells constitutively expressing DsRed for 5 days, then analyzed via flow cytometry. After removing DsRed cells from the data, the level of GFP positivity was unchanged [Fig. 3D]. PCCL3-PPFP cells co-cultured with 4-fold excess control cells also did not lose GFP positivity (data not shown). We conclude that hypothetical activating or inhibiting exogenous ligands are not sufficient for TCF activation, and PPFP activation of TCF pathways occurs via a cell autonomous process.

The PPARγ agonist pioglitazone increases TCF activation.

PCCL3-PPFP cells treated with pioglitazone increased their number of TCF_GFP+ cells by more than two fold [Fig. 4A]. Total changes in cell number were insignificant and not a factor in the increased GFP+ percentage (data not shown). Co-treatment with PPARγ antagonist GW9662 negated the effects of pioglitazone, indicating PPARγ specificity of pioglitazone action. PCCL3-EV control cells were not affected by the treatment. Cells treated with other PPARγ agonists (CAY10410, GW1929) and another PPARγ antagonist (T0070907) yielded similar results (data not shown).

Sorted bulk populations of TCF_GFP- PCCL3-PPFP cells, but not those of PCCL3-EV control cells, saw their TCF_GFP + population increased by pioglitazone to a similar

extent as TCF_GFP+ and unsorted populations [Fig. 4B]. To address the possibility of contaminating TCF_GFP+ cells being responsible for the re-appearance of TCF_GFP+ cells in the TCF_GFP- population, we also treated clonal populations derived from TCF_GFP- cells. These clones had remained TCF unresponsive, previously containing an average of 0.30% TCF_GFP + cells. After treatment with pioglitazone, the clones contained an average of 0.90% TCF_GFP+ cells (n=4, p=0.09), suggestive of a small but real induction of TCF_GFP+ cells from the TCF_GFP- population. The effect of pioglitazone on TCF response is a novel example of a critical stem cell pathway being reactivated in previously negative cells.

The invasiveness of PCCL3-PPFP cells is increased by pioglitazone.

Clonal populations grown from individual cells sorted by their TCF status were treated with pioglitazone or DMSO. Compared to the vehicle treated cells, the pioglitazone treated cells were more invasive, whether derived from TCF_GFP+ or TCF_GFP- cells [Fig. 4C]. The increase was seen in all but 1 of the PCCL3-PPFP clones (n=10). In contrast the two PCCL3-EV control clones tested did not become more invasive with pioglitazone.

The effects of full versus selective PPARγ agonists on PPFP differ in cell culture versus *in vivo*.

The pioglitazone results suggest that exposure of PPFP carcinomas to this drug would likely increase tumor growth and aggressiveness. However, we previously reported that

pioglitazone reduces the growth and metastases of tumors in a transgenic mouse model of PPFP thyroid carcinoma (39). A remarkable feature of those tumors is that pioglitazone caused them to differentiate toward adipocytes, with the cells accumulating large intracellular lipid droplets and inducing a broad array of known PPARγ-inducible adipocyte genes.

We hypothesized that the adipogenic response to pioglitazone and other PPARγ agonists is separable from the increased TCF responsiveness and invasiveness. This hypothesis is potentially testable due to the existence of selective PPARγ modulators (SPPARMs). These small molecules effect the insulin sensitization response of full PPARγ agonists with little to no adipogenesis and other associated side effects of classic agonists such as pioglitazone (120).

We found that SPPARMs also increased the activation of TCF. BVT.13 increased the percentage of TCF responsive cells, and the PPARγ antagonist T0070907 blocked this increase [Fig. 4D]. Similar results were obtained for FMOC-L-Leucine and nTZDpa (data not shown). Each of these reagents was identified as a PPARγ selective agonist with weak adipogenic activity (105; 121–123). The maximal effects of the SPPARMs were volatile despite repeated experiments. We present here experiments demonstrating conservative but statistically significant increases in TCF activation. Other experiments with identical parameters demonstrated increases in TCF_GFP+ percentage similar to pioglitazone treatment.

SR1664 was recently identified as a PPARγ partial agonist with no detectable adipogenic activity (109). It too increased TCF_GFP positivity in PCCL3-PPFP cells [Fig. 4E]. However, PPFP harboring transgenic mice treated with SR1664 received none of the antitumor effect of pioglitazone [Fig. 5], suggesting that the TCF-activating and anti-tumor effects of PPARγ ligands are indeed due to different activities of PPFP.

Taken together, our results suggest the following: 1) PPFP's contribution to malignant transformation depends on its PPARγ DNA and ligand binding domains. 2) PPFP increases the number of TCF responsive PCCL3 cells, a cancer stem cell-like population whose progeny effect the transformed phenotype of PCCL3-PPFP cells. 3) The effects of PPFP are amplified by actions common to PPARγ agonists and non-adipogenic selective agonists *in vitro.* 4) Only the full PPARγ agonist has anti-tumor effects *in vivo*, suggesting that the associated adipocyte transdifferentiation of cancer thyrocytes is more than an incidental effect.

DISCUSSION

PPFP expression occurs in about 35% of FTCs and was one of the first carcinoma-related translocations to be identified, but the molecular mechanisms underlying its role in thyroid carcinogenenesis are not understood. PPFP transforms cells *in vitro* and induces metastatic FTC in mice in conjunction with *Pten* deletion (39; 124), but it also can inhibit growth in already-malignant cell lines and in mouse xenografts of cell lines (125). It

stimulates or inhibits targets of PAX8 and PPARγ depending on the particular gene and cellular context (87–89; 126). Here we report that PPFP via its PPARγ domains activates the Wnt/TCF pathway and that this is an essential step in the transformation effected by PPFP.

Rat thyroid PCCL3 cells expressing PPFP demonstrated higher anchorage-independence and invasive potential. These result are consistent with past reports in other cell lines of the pro-oncogenic effects of PPFP (87–90). PPFP retains the ability to bind PPREs (24; 89) and our data indicate that a functional PPARγ DNA binding domain is required for these actions of PPFP.

We reported previously that PPFP is a potent driver of the PPARγ transcriptional program in the presence of the classic PPARγ agonist pioglitazone (39). We report here that PPARγ agonists enhance the effects of PPFP while PPARγ antagonists block them. Clearly the PPARγ domains of PPFP play an important role in its biology. Selective PPARγ modulators (SPPARMs) also enhance PPFP transformation. We speculate that the oncogenic targets of PPFP are part of a distinct transcriptional program activated by both full and selective PPARγ agonists, rather than the adipogenic program that responds only to the full agonists. *In vivo* in the absence of exogenous ligands the oncogenic action of PPFP dominates and patients or mice develop FTC, but the presence of a strong full agonist such as pioglitazone allows the adipogenic and anti-tumor activities of PPFP to prevail.

Based upon CMAP data, we hypothesized that the Wnt/TCF pathway may be a target of PPFP. Wnt/TCF pathways have a central role in cancer and stem cell biology which is best illustrated by studies in the intestine, where cells with activated Wnt pathways act as stem cells to maintain healthy tissues and drive the progression of malignant disease (76; 77; 79). Wnt pathway activation in the form of β-catenin translocation and TCF reporter stimulation also is observed in all forms of thyroid malignancy but is more common and well studied in papillary and anaplastic thyroid carcinomas than FTC (60; 61; 83; 127).

Expression of PPFP increased the fraction of cells that is Wnt active/TCF responsive, and these cells have properties of cancer stem cells. The TCF responsive and unresponsive fractions are hierarchically organized with the former being able to recapitulate the original heterogeneity in TCF reporter activity while the latter remains wholly unresponsive. The TCF responsive fraction is also enriched for invasive and colony forming cells. Our data suggest that PPFP exerts its oncogenic effects on the small fraction of stem and progenitor like cells in the thyroid, effects that may be obscured when only the bulk population is examined. Thus, the reporter assays we used to identify a functionally significant subpopulation of thyroid cancer cells are promising tools for future use in the study of thyroid stem cells and cancer stem cells.

The functional relationship between PPFP and PPARγ is decidedly unsettled; our data suggest hypotheses that may help resolve the discrepancies. We have previously shown

that PPFP induces some PPARγ target genes while repressing others, but with agonist activation adipocyte PPARγ target genes are broadly upregulated by PPFP in the mouse thyroid (39). Here we demonstrate that the transforming effects of PPFP in PCCL3 cells are enhanced by PPARγ agonists and blocked by PPARγ antagonists. This is in contrast to the prevailing hypothesis that PPFP uniformly acts as a dominant negative PPARγ thus blocking PPARγ's putative tumor suppressive properties. However our results are more consistent with observations that PPARγ and its agonists increase the tumorigenicity of anaplastic thyroid carcinoma cells (128).

Evidence of PPARγ suppression by PPFP has been collected in cell systems with significant PPARγ activity, while in the normal human thyroid and FTC PPARγ expression is barely detectable. PPFP suppresses PPARγ activity in osteosarcoma cells, HeLa cervical carcinoma cells, and NIH3T3 fibroblasts (87–89). PPFP also suppresses PPARγ transactivation in immortalized thyroid Nthy-ori cells, but the endogenous level of PPARγ in these cells is not insignificant (88). On the other hand, PPFP stimulates PPAR response elements in FRTL5 thyroid cells with very low PPARγ expression (24; 89).

Since the transcriptional program of PPFP includes some PPARγ target genes, we speculate that decreased PPARγ transcriptional activation in the presence of both PPFP and PPARγ could reflect mutual antagonism between the two proteins. The expression of PPFP in PPARγ expressing cells could upset the equilibrium between PPARγ and its

binding partners, co-activators and co-repressors, leading to decreased stimulation of PPREs, especially in the absence of strong exogenous agonists such as pioglitazone. Similarly, competition from PPARγ may disrupt PPFP's own transcriptional program. Such a relationship may also explain why PPFP or similar PPARγ fusions have not been found in other cancers. Low endogenous PPARγ levels such as found in the thyroid may be necessary for the full oncogenic effects of PPARγ fusion proteins.

In conclusion, we identified the Wnt/TCF pathway as a major positively regulated target of PPFP in stably transfected PCCL3 thyroid cells. PPFP activation of the TCF pathway depends on its functional PPARγ DNA and ligand binding domains and can be modulated by small molecules in a PPARγ like manner. The fraction of cells that is TCF responsive due to PPFP activity has the *in vitro* properties of cancer stem cells, suggesting that PPFP-driven Wnt/TCF pathway activation may be an important driving factor in the development of this carcinoma, and hence also may be a therapeutic target.

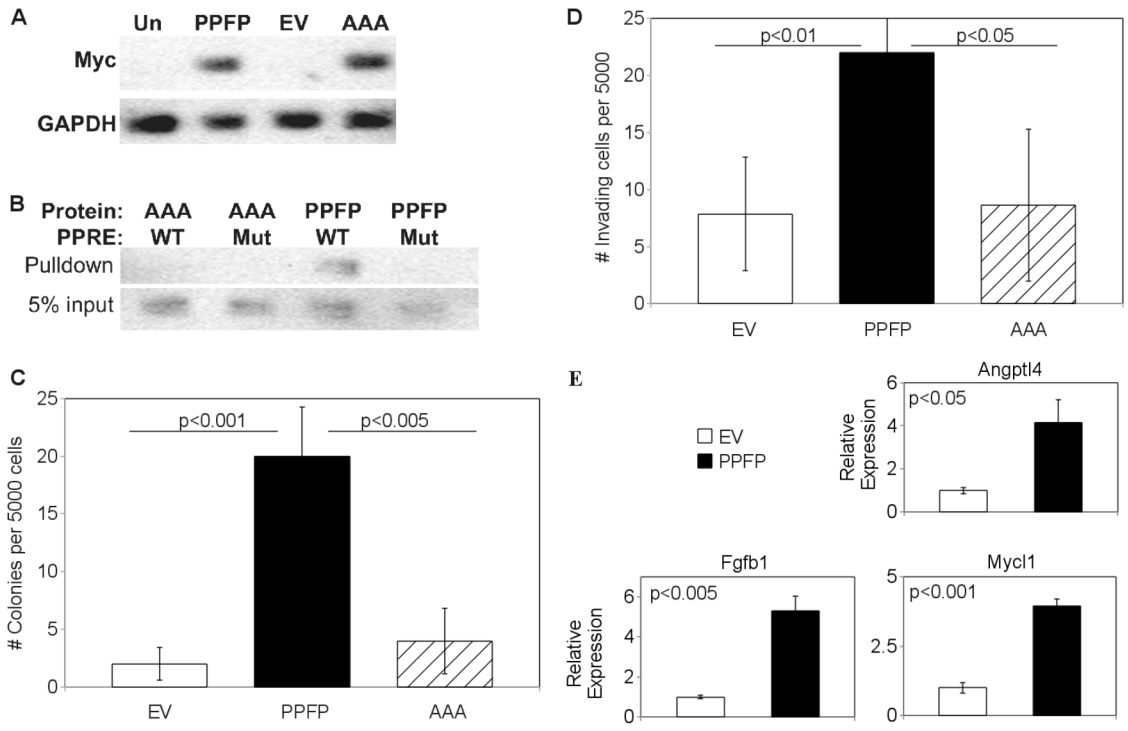

Figure 2.1. (A) Expression of PPFP in stably transfected PCCL3 cells. Whole cell lysates were made from untransfected PCCL3 cells (Un), or PCCL3 cells stably transfected with either PPFP, empty vector (EV), or PPFP in which the P Box amino acids EGG were mutated to AAA (AAA). Twenty micrograms of protein per lysate were analyzed by Western blot for Myc, after which the blot was reprobed for GAPDH. PPFP is ~100 kDa and GAPDH is ~36 kDa. (B) P Box mutation AAA prevents binding of PPFP to a PPAR response element (PPRE). PCCL3-PPFP or PCCL3-AAA whole cell lysates were incubated with a biotinylated PPRE from the mouse Aqp7 gene (WT) or a mutated version (Mut), as described in Methods. Protein-DNA complexes were isolated with NeutrAvidin agarose beads and were analyzed for PPFP by Western blot using anti-Myc (top row). Five percent of input also was analyzed (bottom row). (C) Increased soft agar colony formation by PCCL3-PPFP cells. PCCL3-EV, -PPFP or -AAA cells were suspended in soft agar at 5000 cells per well and colony formation after 21 days was determined as described in Methods. Results are expressed as means ± SD and repeated with independent cell lines. (D) Increased invasion by PCCL3-PPFP cells. PCCL3-EV, -PPFP, or –AAA cells were plated on Matrigel-coated transwells with serum-free media and placed in tissue culture wells containing 10% FBS as attractant. After 36 hours, cells that invaded through the transwell membrane were counted under a microscope. Results are expressed as means ± SD and repeated with independent cell lines. (E) Upregulation in PCCL3-PPFP cells of genes overexpressed in human PPFP FTC. Five genes common to 2 published profiles of genes overexpressed in human PPFP FTC were analyzed by RT-qPCR in lysates from PCCL3-EV and PCCL3-PPFP cells. The 3 genes shown here

had increased expression in the PCCL3-PPFP cells; the other two genes had no change (data not shown). Results are means ± SD.

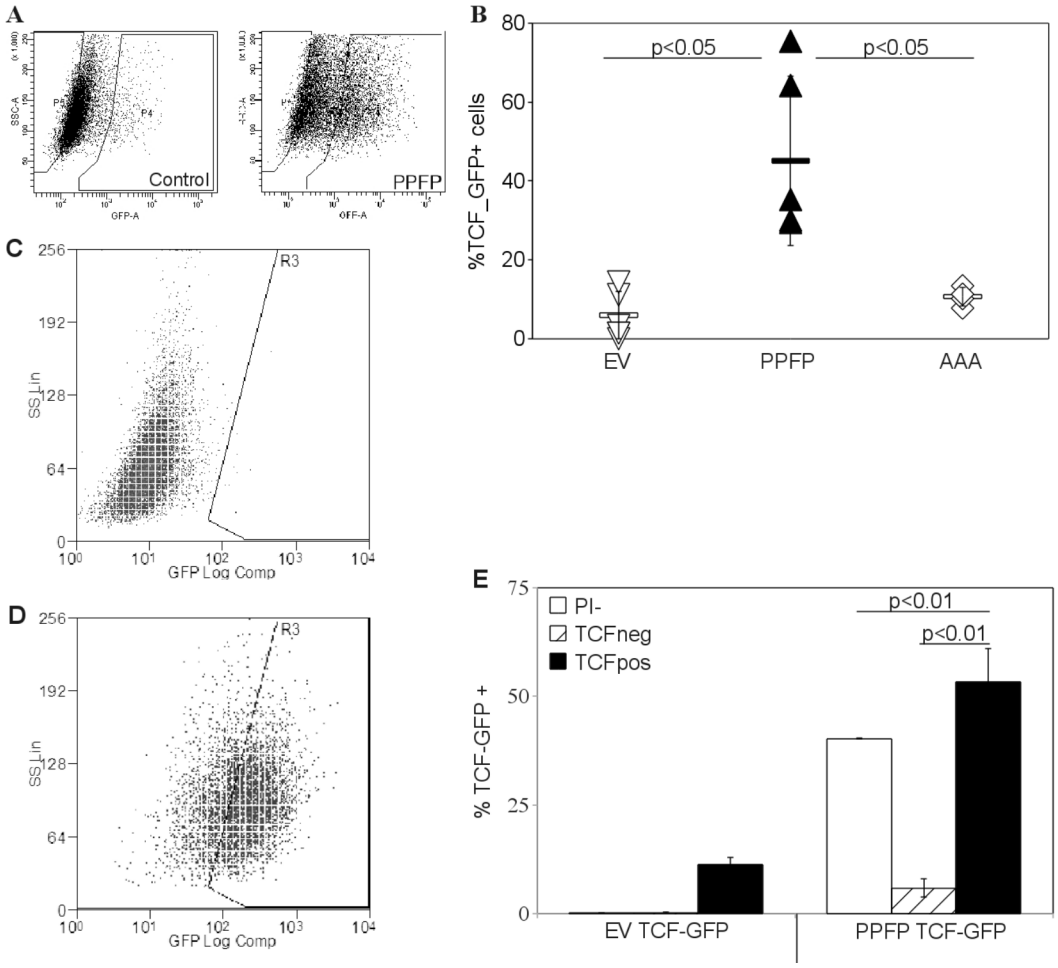

Figure 2.2 (A) Increased TCF driven GFP expression in PCCL3-PPFP cells. Empty vector control PCCL3 and PCCL3-PPFP cells were infected with lentiviral constructs carrying a GFP gene driven by a TCF responsive promoter. Cells which expressed GFP after 5 days in culture were sorted out and expanded to create 100% transfected cell lines. These cell lines were analyzed for GFP expression by flow cytometry. Gates were set at the level of GFP expression in 99.5% of control cells expressing GFP under the control of the same promoter without TCF response elements. Test samples with GFP levels higher than gated were considered GFP positive and TCF responsive. (B) Increased TCF_GFP positivity in multiple PPFP cell lines versus empty vector control and AAA cells. Empty vector control PCCL3-EV, PCCL3-PPFP, and PCCL3-AAA cell lines were infected with the TCF reporter construct as described in (A) and analyzed via flow cytometry. Each point on the graph represents an independent cell line. Results are typical of many (>3) repeated experiments. (C, D) Re-establishment of TCF heterogeneity by TCF_GFP+ cells. The GFP+ and GFP- fractions were placed in cultur

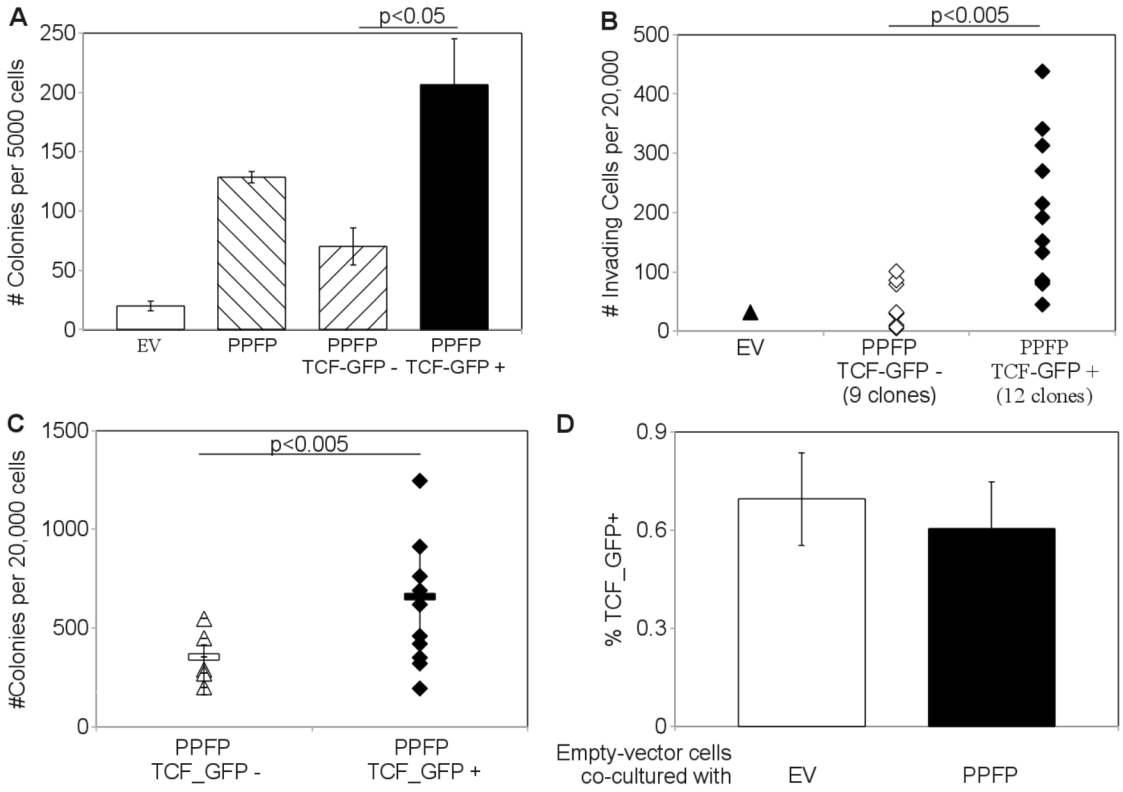

Figure 2.3. (A) Increased Soft agar colony formation in TCF_GFP+ cells. PCCL3-PPFP cells were sorted via FACS into 3 separate samples: whole population (gated on viability only, labeled PPFP on graph), TCF-GFP-, and TCF-GFP+ (gated on viability and GFP). 5000 cells from each sample were suspended and cultured in 0.33% agarose and analyzed for colony formation after 21 days. (B) Increased soft agar colony formation in cell lines derived from single TCF_GFP+ cells. Cell lines were established from individual cells. The TCF status of the founding cells is indicated below the X-axis. 20,000 cells from each clonal cell line were suspended and cultured in 0.33% agarose and analyzed for colony formation. (C) Increased invasion through Matrigel by cell lines derived from individual TCF_GFP+ cells. The TCF status of the founding cells is indicated below the X-axis. 20,000 cells from each clonal cell line were placed in a Matrigel-coated transwell and analyzed for invasion after 36 hours. (D) No increase in TCF activation despite co-culture with PPFP cells. Empty vector control PCCL3-EV cells were co-cultured with 4 fold excess PCCL3-EV or PCCL3-PPFP constitutive-DsRed cells. After 5 days in culture the cells were analyzed for GFP status by flow cytometry. During analysis, DsRed positive cells were excluded so that the % TCF_GFP+ reported is from the DsRed negative PCCL3-EV cells only. Columns represent means ± SD; the experiment was repeated and similar results obtained.

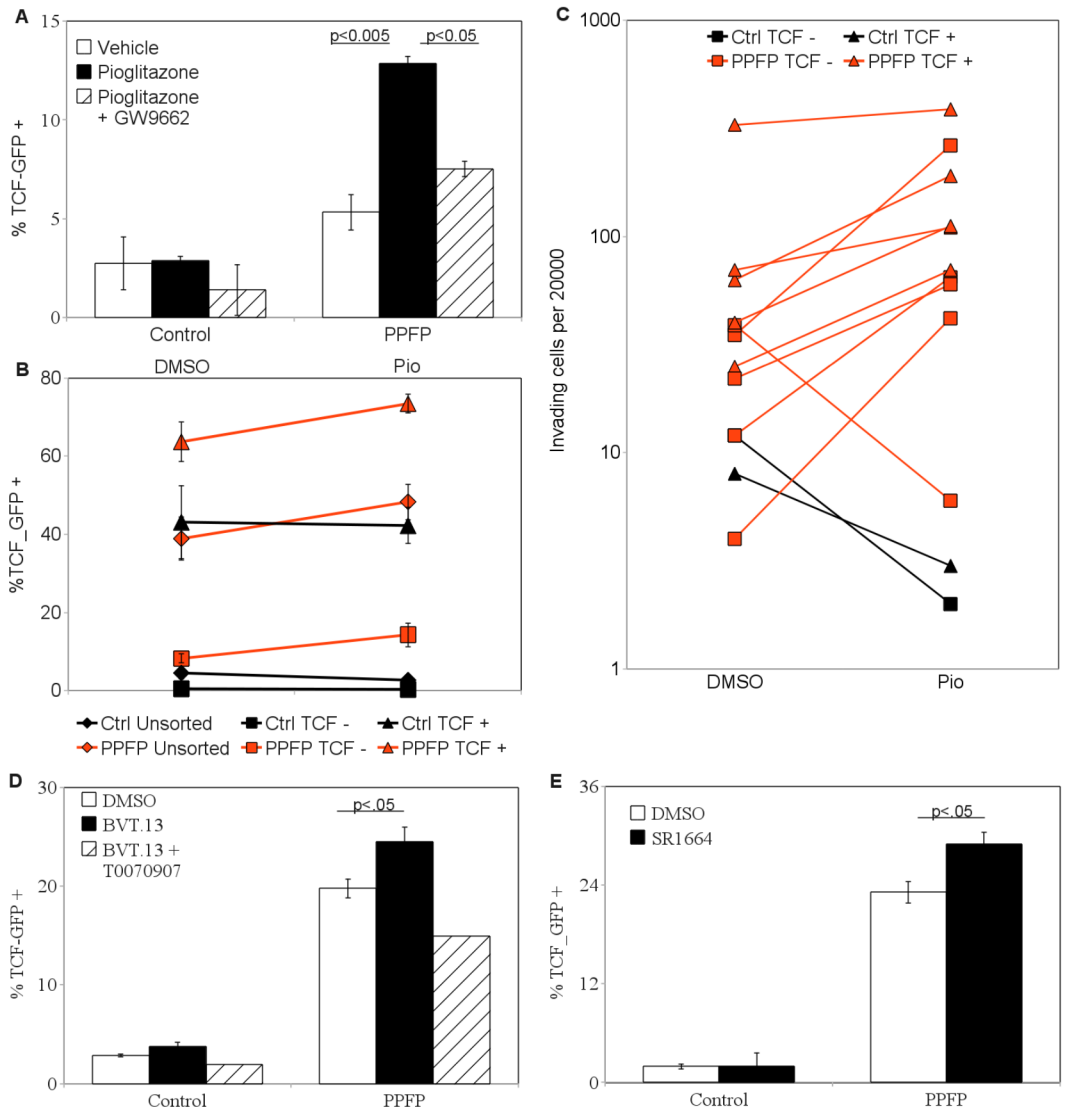

Figure 2.4. (A) Increased TCF activation after pioglitazone treatment. PCCL3-EV and PCCL3-PPFP cells were treated with the PPARγ agonist pioglitazone (1μM) with or without the PPARγ antagonist GW9662 (0.1μM) for 5 days. The cells were then analyzed via flow cytometry for GFP status. (B) Increased TCF activation in each pioglitazone treated fraction of the PCCL3-PPFP cell line. PCCL3-EV and PCCL3-PPFP cells were sorted via FACS into whole population, TCF_GFP-, and TCF_GFP+ samples. The sorted cells were cultured for 5 days in the presence of pioglitazone (1μM) or vehicle (DMSO). Cells were then analyzed via flow cytometry for GFP status. (C) Increased invasiveness of pioglitazone treated PPFP cell lines. Cell lines each derived from a single TCF_GFP- or TCF_GFP+ cell were treated with pioglitazone (1μM) for 5 days. Cells were then placed in Matrigel-coated transwells and their invasive capacities were analyzed. PPFP

expressing cells were more invasive with pioglitazone treatment regardless of whether they were from a GFP- or GFP+ cell. (D) Increased TCF activation by a selective PPARγ agonist. Empty vector control and PCCL3-PPFP cells were treated for 5 days with the selective PPARγ agonist BVT.13 (1μM) with or without the PPARγ antagonist T0070907 (1μM). Cells were then recovered and analyzed via flow cytometry for GFP status. (D) Increased TCF activation by non-adipogenic selective PPARγ agonist. PCCL3-EV and PCCL3-PPFP cells were treated for 5 days with the non-adipogenic selective PPARγ agonist SR1664 (1μM). Cells were then recovered and analyzed via flow cytometry for GFP status.

Figure 5. SR1664 does not inhibit thyroid tumor growth in vivo. Mice with thyroid-specific expression of PPFP and Pten deletion were treated with control diet, pioglitazone, or the selective PPARγ agonist SR1664 for two weeks starting at age 8 weeks. Thyroid size was measured by ultrasound at the start and end of treatment. Each line represents one mouse. Thyroid area of wild type mice is 1.9 mm2 and does not change over the two week period (data not shown).

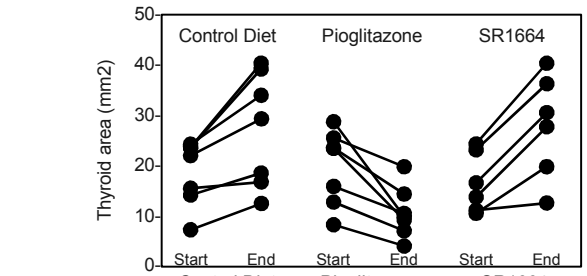

	Control Diet	Pioglitazone	SR1664
Start Area (mm2):	18.5±6.5	19.1±7.5	16.4±5.9
End Area (mm2):	26.8±11.4	10.7±5.0	27.6±10.4
Fold Change:	1.44±0.24	0.57±0.15	1.68±0.32
N:	7	7	6

Figure 2.5. SR1664 does not inhibit thyroid tumor growth in vivo. Mice with thyroid-specific expression of PPFP and Pten deletion were treated with control diet, pioglitazone, or the selective PPARγ agonist SR1664 for two weeks starting at age 8 weeks. Thyroid size was measured by ultrasound at the start and end of treatment. Each line represents one mouse. Thyroid area of wild type mice is 1.9 mm2 and does not change over the two week period (data not shown).

ACAA1, ALDH1L1, ANGPTL4, AQP7, CHIA, CXCR7, DHCR24, ENO3, PMP22, FBN2 , FBP1, FGFBP1, MYCL1, PPARG, RAB15, TNFRSF21, XK

Table 2.1. Genes in common between the expression profiles of PPFP thyroid carcinomas identified by Lacroix et al. (105) and Giordano et al. (24).

rank	cmap name	dose	cell	score	up	down
111	pioglitazone	10 μM	PC3	0.841	0.393	-0.743
228	pioglitazone	10 μM	PC3	0.793	0.399	-0.672
259	pioglitazone	10 μM	PC3	0.786	0.245	-0.817
501	pioglitazone	10 μM	MCF7	0.73	0.308	-0.678
599	pioglitazone	10 μM	MCF7	0.713	0.139	-0.824
648	pioglitazone	10 μM	PC3	0.705	0.277	-0.676
1141	pioglitazone	10 μM	PC3	0.625	0.222	-0.623
2191	pioglitazone	10 μM	MCF7	0	0.236	0.598
2240	pioglitazone	10 μM	MCF7	0	0.229	0.718
3349	pioglitazone	10 μM	MCF7	0	-0.118	-0.681
5816	pioglitazone	10 μM	MCF7	-0.783	-0.144	0.89

Table 2.2. Connectivity Map results showing the congruence of the common PPFP profile and gene expression changes caused by pioglitazone treatment. Each row represents an CMAP instance - a treatment and control pair subjected to gene expression profiling to derive a set of differentially expressed genes. The score is a value between 1 and -1 indicating the level of overlap between a CMAP instance and the query signature. A high positive score indicates a treatment which induced a set of gene expression changes similar to the query. A low negative score indicates a treatment which reversed the gene expression changes in the query. A 0 score indicates no self-consistent correlation between the two sets. The up and down columns indicate the enrichment scores for the induced and repressed gene set, respectively. Considering all 11 instances together, pioglitazone induced genes were enriched in the common PPFP profile ($p = 0.014$, as calculated by CMAP).

name	mean score	n	enrichment	p	specificity	% non-null
verteporfin	-0.851	3	-0.969	0.00008	0.0058	100
colforsin	0.481	5	0.725	0.00364	0.0101	80
hymecromone	-0.479	4	-0.749	0.0079	0.0121	75
bisacodyl	-0.615	4	-0.748	0.00812	0.0403	75
simvastatin	0.6	4	0.742	0.00849	0.0247	100
amiloride	-0.603	5	-0.668	0.00953	0.0052	80
altizide	-0.315	4	-0.691	0.01971	0.0131	50
methotrexate	0.397	8	0.507	0.02008	0.1024	62
azacitidine	0.606	3	0.781	0.02119	0.1394	100
securinine	-0.584	4	-0.674	0.02524	0.1456	75
proadifen	-0.584	4	-0.671	0.02616	0.0261	75
merbromin	-0.345	5	-0.605	0.0272	0.1707	80
anisomycin	-0.498	4	-0.661	0.02988	0.1864	75
digoxin	-0.549	4	-0.659	0.03079	0.1122	75
lycorine	-0.379	5	-0.581	0.03827	0.28	60
fluspirilene	0.556	4	0.635	0.04372	0.1005	75

Table 2.3. Small molecules which elicited similar gene expression changes to the common PPFP profile, which were also Chembank HTS standard hits for Wnt inhibitor, Wnt/Lithium modulators, or β-catenin inducer/translocator. Mean score is the average connectivity score of control-treated pairs for a molecule in the CMAP database, n indicates the number such pairs. Enrichment indicates the relative connectivity of a particular set of instances compared against all other instances. Specificity indicates the relative uniqueness of connectivity by tallying the frequency at which the connectivity between the query and relevant instances is equaled or exceeded by the connectivity between the same instances and a large number of gene signatures from MSigDB. Non-null percentage refers to the number of instances that are scored in the same direction as the majority instances.

CHAPTER 3

Establishing cell lines and an immune competent syngeneic tumor initiation model from PPFP/PTENthy-/- mice.

Transgenic mice expressing PPFP and missing PTEN due to thyroid specific double knockout spontaneously develop metastatic thyroid carcinoma (39; 124). Cells recovered from these tumors present two unique research opportunities: the development of the first PPFP follicular thyroid carcinoma cell lines, and the development of a tumorigenicity assay to test cancer stem cells in immune competent, syngeneic mice.

PPFP+/PTEN-/- FTC cells were separable from the surrounding tissues on the basis of fluorescence. PPFP+/PTEN-/- cells were GFP negative against the background of constitutive GFP positivity in other cells. Cells from thyroid tumors consisted of 50% GFP- tumor cells and 50% GFP+ others [Fig. 3.1A]. Cells from metastases consisted of 90% GFP- tumor cells [Fig. 3.1B].

The GFP- tumor cells were sorted and expanded in culture to establish a heterogenous population. The dissociated cells required Matrigel coated plates to grow well initially,

but were able to proliferate on treated plastic after passage 5 [data not shown]. EGF and TSH together provided the stimulation that allowed the cells to proliferate [Figs. 3.1C, 3.2].

The collected and cultured cells contained a TCF responsive sub-population. The collected cells were checked to ensure that they remained GFP negative before being transfected with one of two TCF reporter constructs driving GFP expression. GFP positive cells were isolated and expanded to create 100% transfected cell lines. Using either construct on independent collections of tumor cells, we found between 3-12% TCF responsive cells [Fig. 3.3A].

The PPFP+/PTEN-/- cells responded to PPARγ agonist treatment and harbor a TCF based hierarchy like PCCL3_PPFP cells. Pioglitazone treatment increased TCF activation by 2 fold at 1μM and by 4 fold at 5μM [Fig. 3.3B]. Clones derived from TCF_GFP+ cells regenerated both the TCF heterogeneity of the original cell lines, while the majority of clones derived from TCF_GFP- cells remained wholly negative. Two of the TCF_GFP- clones regenerated a small number of TCF_GFP+ cells [Fig. 3.3C].

Unfortunately, these cultured cells did not form tumors when injected into FVBN mice. Perhaps being kept in culture had adversely affected their tumorigenicity since freshly dissociated cells readily formed tumors in syngeneic, immune competent FVBN mice.

Subcutaneous injections of 10^6 unsorted cells readily formed tumors in FVBN mice [Tab. 3.1, Fig. 3.4A-C]. When recovered, the tumors were devoid of GFP+ cells, suggesting that only PPFP+/PTEN-/- cells from the unsorted tumors grew in the host mouse [data not shown]. Cells recovered from subcutaneous tumors were injected into new mice and again formed tumors, demonstrating passageability [Fig. 3.4D].

We are working to optimize a protocol for transfecting the dissociated tumors with constitutive DsRed TCF reporter vectors. DsRed will allow the specific recovery of tumor cells via for passaging studies. With this we will have a platform to assay tumorigenicity and self renewal in an immune competent mouse model, using cells which have never been in culture.

Materials and Methods

Mouse Procedures

Mouse breeding and all procedures involving live mice were conducted in accordance with standard operating procedures approved by the University Committee on the Use and Care of Animals at the University of Michigan. PPFP+/PTEN$^{thy-/-}$ mice were bred as previously described (39; 124). Mice with thyroid tumors were anesthesized and killed using ketamine/xylazine.

Subcutaneous injections of tumor cells were made into the flank of FVBN mice. Cells to be injected were suspended in 200ul of 50% matrigel in HBSS.

Obtaining Single cells from Mouse Tumors.

Tumor tissues were minced then enzymatically dissociated with collagenase/hyaluronidase (Stemcell Technologies) in DMEM. Red blood cells were lysed with NH_4Cl treatment. Tumor cell suspension was filtered through 40 micron sieve to obtain single cells.

Cell Culture

Mouse tumor cells were grown at 5% CO_2 in Coon's F-12 media identical to those used for PCCL3 cells, supplemented with 10nM mEGF.

Cell numbers were counted by diluting 100µl in 10ml PBS and the resulting cell suspension run through a Coulter counter (Beckman Coulter). Cell debris was discarded from analysis by Coulter counter software.

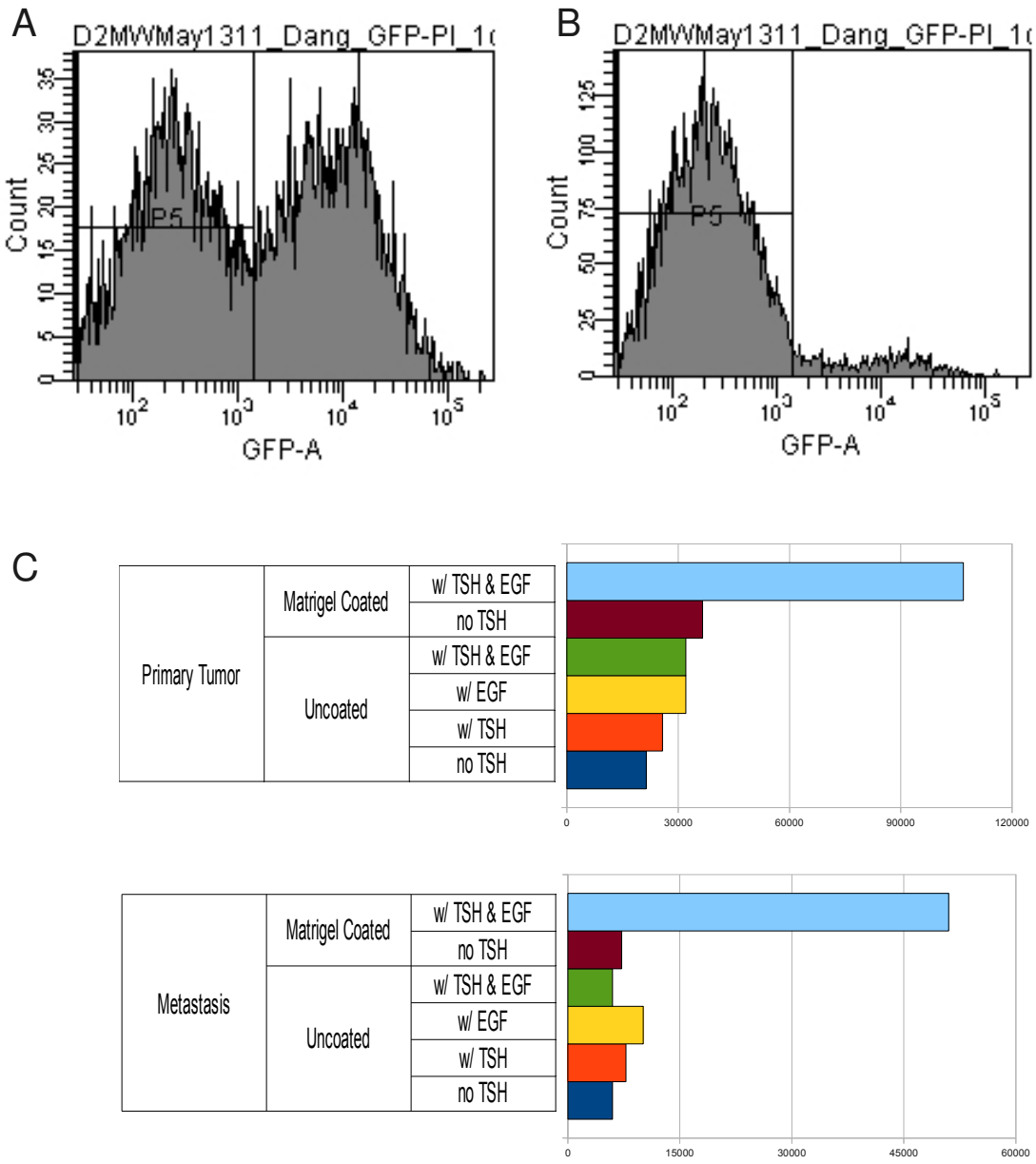

Figure 3.1. (A) PPFP/PTENthy-/- cells in dissociated mouse thyroid tumors. PPFP/PTENthy-/- cells were GFP- (indicating successful Cre activity) while all other cells in the transgenic mouse were GFP+. Spontaneous thyroid tumors were dissociated with collagenase/hyaluronidase and filtered through a 40 micron mesh to eliminate aggregates. Red blood cells were lysed with NH_4Cl and the remaining single cells collected analyzed via flow cytometry. (B) PPFP/PTENthy-/- cells in dissociated spontaneous metastasis. Single cells were collected from a subcutaneous metastasis in the same mouse as (A). (C) PPFP/PTENthy-/- cell growth in culture. Thyroid and metastatic tumors were dissociated as before. GFP- (PPFP/PTENthy-/-) cells were isolated via FACS. Equal number of dissociated tumor cells were started on matrigel coated or tissue

culture plastic plates in Coon's F-12 media + FBS, insulin, apo-transferrin, and hydro cortisone. EGF and/or TSH were also added to the media. After 5 days in culture, cells were trypsinized and counted with a Coulter counter.

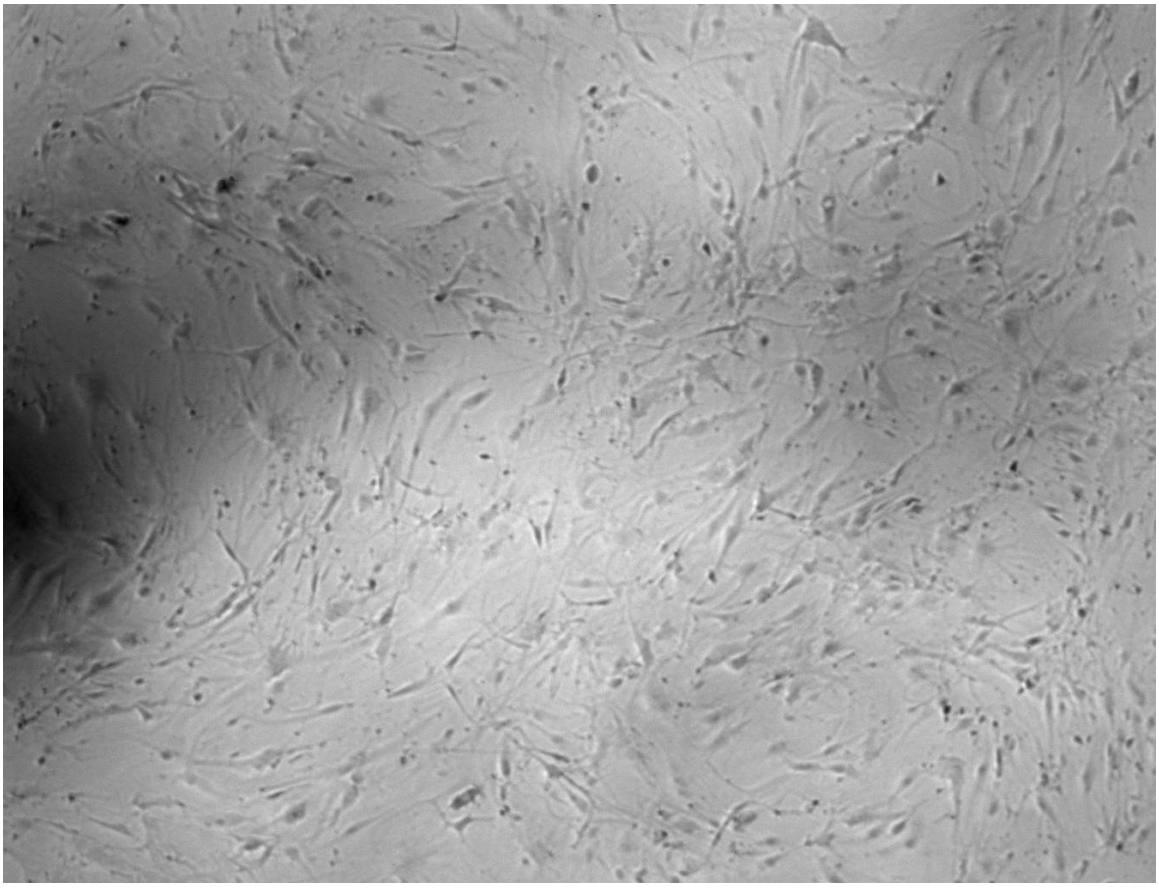

Figure 3.2. Cells from dissociated PPFP+/PTEN-/- tumors growing on Matrigel coated plates. Cells from primary thyroid and metastatic tumors were dissociated and sorted for GFP negativity, indicating successful Cre activity. PPFP/PTENthy-/- cells were grown on Matrigel coated plates in Coon's F12 media supplemented with 4H (insulin, hydro cortisone, apo-transferrin, TSH) cocktail and EGF. Cells depicted are in their 3rd passage.

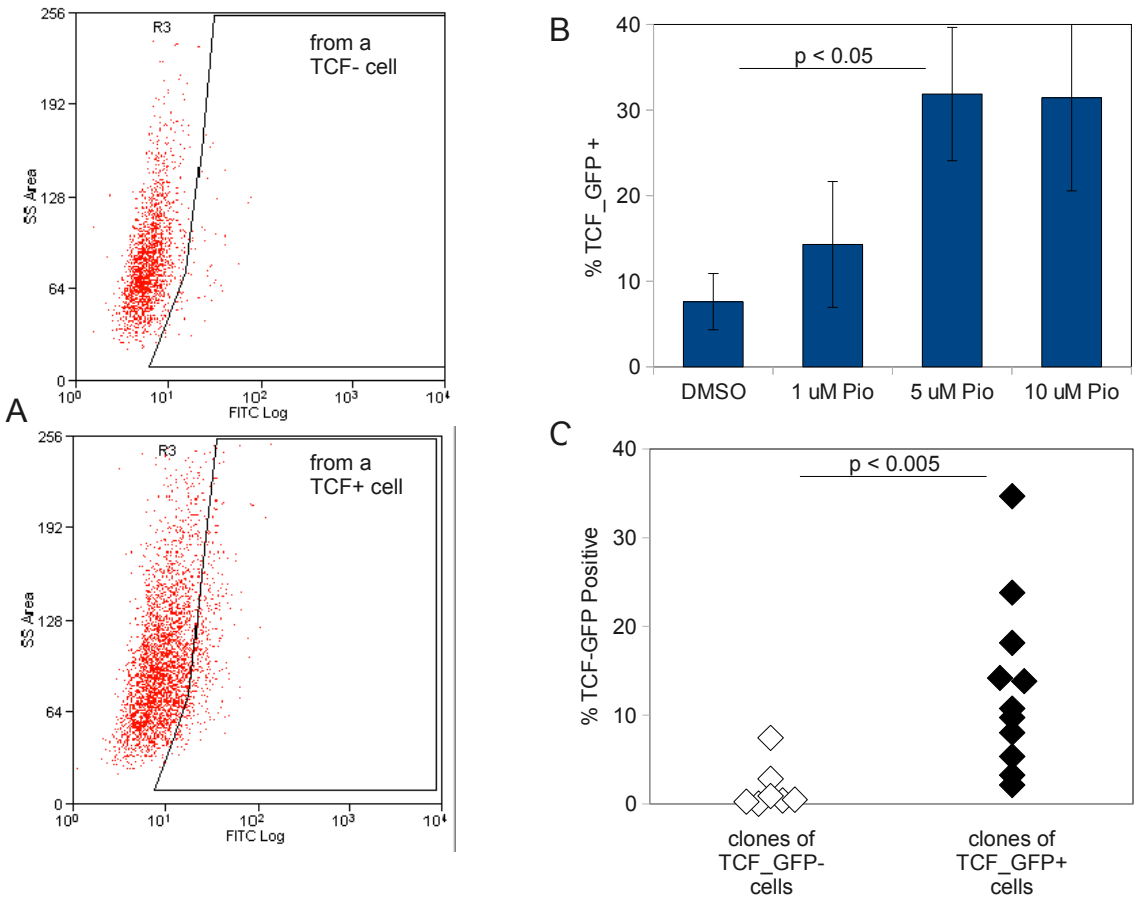

Figure 3.3. (A) TCF activation in PPFP/PTEN-/- cells. After delivery of TCF_GFP reporter constructs via lentivirus, GFP positive cells were sorted out and expanded to create 100% transfected cell populations. These populations regenerated TCF_GFP- and + cells as they grew and eventually contained from 3 to 12% TCF_GFP+ cells (top and bottom respectively). (B) Dose dependent increase in TCF activation after Pioglitazone treatment. Cells expressing GFP under a TCF responsive promoter were treated with DMSO (vehicle control) or pioglitazone at 1, 5, or 10μM. After 5 days of treatment cells were removed from culture and analyzed via flow cytometry. Results are means ± SD and were repeated with independent cell lines. (C) Re-establishment of TCF heterogeneity by TCF_GFP+ clones. A single cell was sorted into each well of a 96 well plate. The cells were sorted by their GFP status. Single cells which grew into robust, passageable cell lines were collected for further studies. Clones of TCF_GFP+ generated heterogenous populations with varying TCF_GFP+ fractions. Most clones of TCF_GFP- cells remained negative, while a small fraction of the clones regenerated a low level of the TCF_GFP+ fraction.

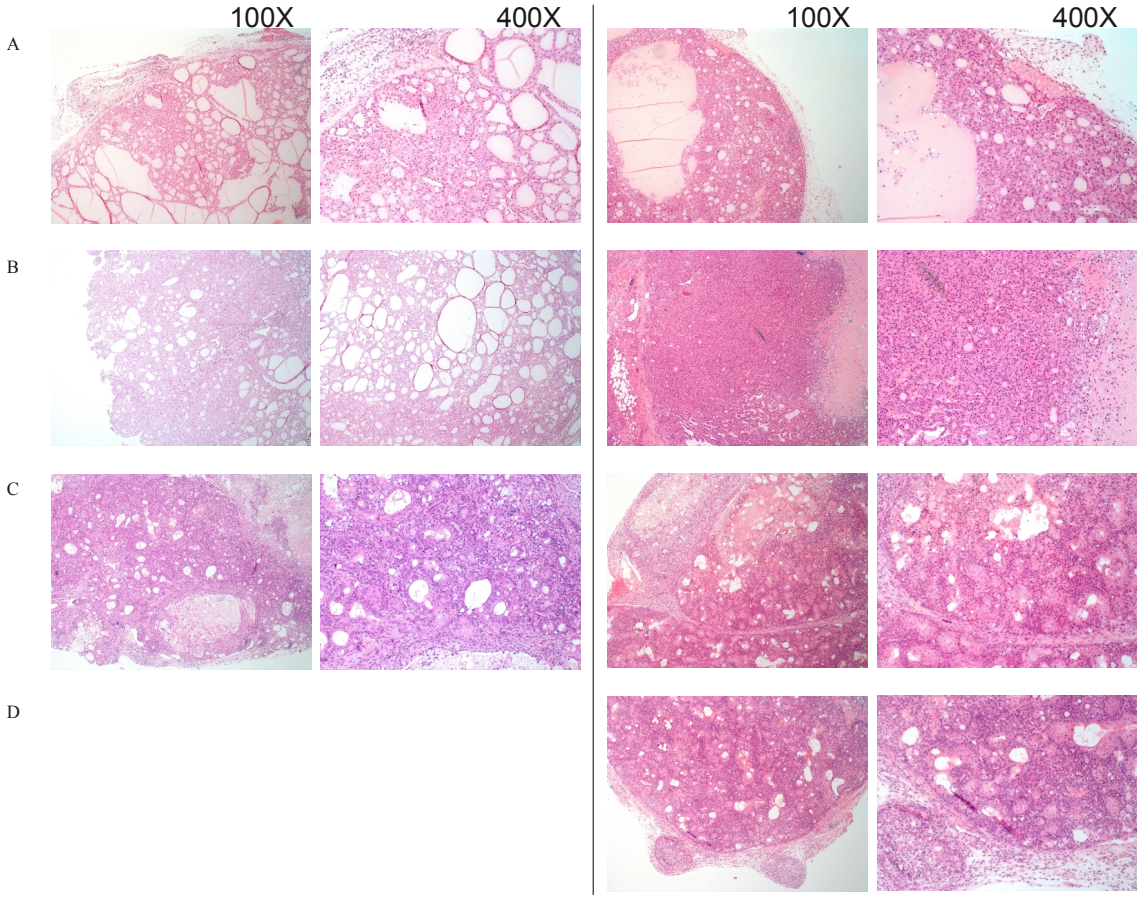

Figure 3.4. H&E stained sections of spontaneous tumors from PPFP+/PTEN$^{thy-/-}$ mice (A-C left) and subcutaneous tumors that grew when FVBN mice were injected with cells collected by dissociating the respective spontaneous tumors on the left (A-C right). The tumor in D arose from cells collected from the subcutaneous tumor in C-right and injected into a new FVBN mouse.

Tumor Site	Injections (10^6 cells at each)	Tumors formed
Primary	3	2
Metastasis	2	2
Subcutaneous, from injections	4	4

Table 3.1. Summary of tumor forming efficiency. PPFP/PTENthy-/- tumors were dissociated to obtain single cells. 10^6 cells were suspended in 50% Matrigel and injected subcutaneously into the flank of FVBN mice. Mice were observed up to a year after injection for tumor formation. Time until tumor grew to experiment endpoint (1cm diameter) was 173 ± 52 days for primary tumors, 117 ± 28 days for metastases, and 85 days for passaged tumors.

CHAPTER 4

PPFP expression increased ALDH activity and sphere formation

Aldehyde dehydrogenase (ALDH) was first discovered as a marker for hematopoietic stem cells and was later found to be elevated in solid tumor and non-hematologic tissue stem cells as well (49; 53; 129). Aldefluor is an enzymatic assay which generates fluorescence by cellular retention of undiffusible- when-cleaved fluorescent substrates of aldehyde dehydrogenase; high levels of ALDH activity leads to brighter cells. (51). Like in many other tissues, the aldefluor bright fraction has been reported to contain the tumorigenic and metastatic cancer stem cells in the thyroid (54).

Increased ALDH expression was observed in human PPFP+ FTC samples. In tissue samples of human FTC expressing PPFP, we observed a sizable fraction of cells stained for ALDH compared to very few in the normal thyroid [Fig. 4.1]. There are no human PPFP FTC cell lines. We examined instead the human FTC-236 and FTC238 cell lines, both of which overexpress PPARγ but without apparent PPARγ fusion proteins (103; 130). Distinct fractions of the cell lines were Aldefluor bright [Fig. 4.2A]. Aldefluor bright cells formed more colonies in a serum free suspension culture [Fig. 4.2B]. Spheres

formed in these assays were collected, dissociated, and passaged. Cells from Aldefluor bright spheres were vastly more capable of forming 2^o and 3^o spheres [Fig. 4.2B,C]. This suggested the Aldefluor bright cells in FTC cell lines were more capable of long term self renewal.

PCCL3_PPFP cells expressed 9 times more ALDH1A1 compared to empty vector control [Fig 4.3A]. This increase in ALDH expression accompanied a two fold increase in Aldefluor bright cells [Fig 4.3B,C]. Unlike the TCF responsive cells, however, clones derived from single cells sorted by Aldefluor status readily regenerated the Aldefluor heterogeneity of the original population regardless of their original Aldefluor status [Fig. 4.3D]. Neither Aldefluor bright nor dim clones exhibited exclusive bipotential capacity, leading us to believe that TCF responsive cells may be a more specific strategy to enrich for cancer stem cells.

We also observed higher colony formation in serum free suspension culture by PCCL3_PPFP cells compared to empty vector control. The rate of colony formation was dependent on viscosity of the suspension media, suggesting that aggregation played a role. An experiment in which equal number of DsRed and GFP fluorescent PCCL3 cells were co-cultured in suspension demonstrated that only 20% of the spheres were single-color, meaning the vast majority of the spheres arose from more than one cell. Single cells sorted into individual wells failed to form spheres. We made note of PCCL3's possible requirement for juxtacrine signalling in serum free condition and subsequently

we used the classical soft agar assay to probe PPFP's effects on anchorage independent proliferation.

PPFP expression increased the percentage of Aldefluor bright cells which have some *in vitro* properties of CSCs but not others. The data showing Aldefluor negative cells regenerating Aldefluor bright cells may indicate that in PCCL3_PPFP Aldefluor is not as specific a strategy to enrich for cancer stem cells as the TCF reporter system. Nonetheless, tumorigenicity assays *in vivo* remain to be done for either system.

Materials and Methods

Cell Culture

FTC236 and FTC238 cell lines were cultured at 10% CO_2 in DMEM and Ham′s F12 both with L-Glutamine (1:1 mixture) supplemented with 10% fetal bovine serum, 10µg/ml Insulin, 0.01U/ml Thyroid Stimulating Hormone (TSH), pennicilin and streptomycin.

Histology

Paraffin-embedded sections were deparaffinized in xylene and rehydrated in graded alcohol. Antigen retrieval was accomplished by incubating the sections in citrate buffer pH 6 at 98º. ALDH1 antibody (BD biosciences) was used at a 1/100 dilution. Staining was done using Peroxidase histostain-Plus Kit (Zymed). AEC (Zymed) was used as a substrate for peroxidase. Slides were counter-stained with hematoxylin and coverslipped with glycerin.

Aldefluor Assay

Cells with high ALDH activities were identified using the Aldefluor kit according to the manufacturer's protocol. Cells were suspended in Aldefluor buffer containing the channel blocker verapamil (50μM), an ALDH fluorescent substrate BAAA (1μM), with or without an ALDH inhibitor DEAB (50mM). Cells were incubated for 40 minutes at 37^{o} during which time any BAAA cleaved by ALDH becomes indiffusible and retained inside the cells. Cells were washed HBSS, resuspended in HBSS with PI or DAPI for viability discrimination, and analyzed on a flow cytometer. Cells incubated with DEAB served as negative control and were used to set the gate to determine Aldefluor bright/positivity.

Sphere Assay

Dissociated single cells, after checking and counting on a hemocytometer, were placed in serum free suspension culture as previously described (131): 5000 cells per ml (FTC cells) or 500 cells per ml (PCCL3) were resuspended in DMEM/F12 media supplemented with 10 ng/ml EGF, 10 ng/ml bFGF, 4μg/ml heparin, B27 supplement (Invitrogen). Spheres were collected on a 40 micron sieve to discard single cells and dissociated with trypsin. Dissociated cells were replaced in serum free suspension culture as before.

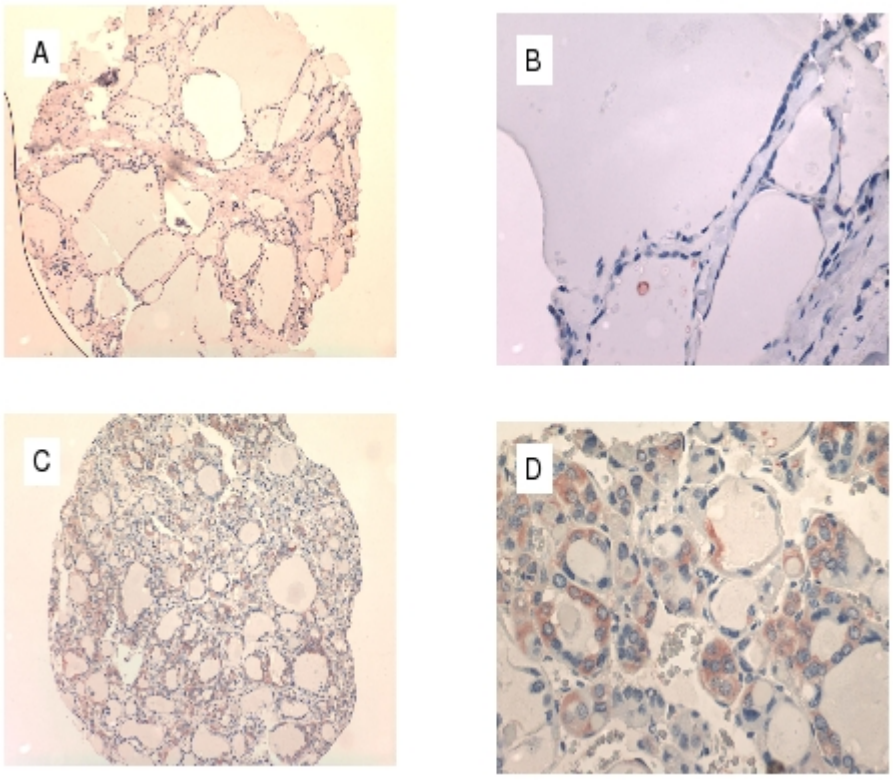

Figure 4.1. ALDH staining of typical tissue microarray samples. ALDH staining of typical tissue microarray samples of normal thyroid tissue (A, at 100X and B at 400X) and PPFP expressing FTC (C at 100X, D at 400X).

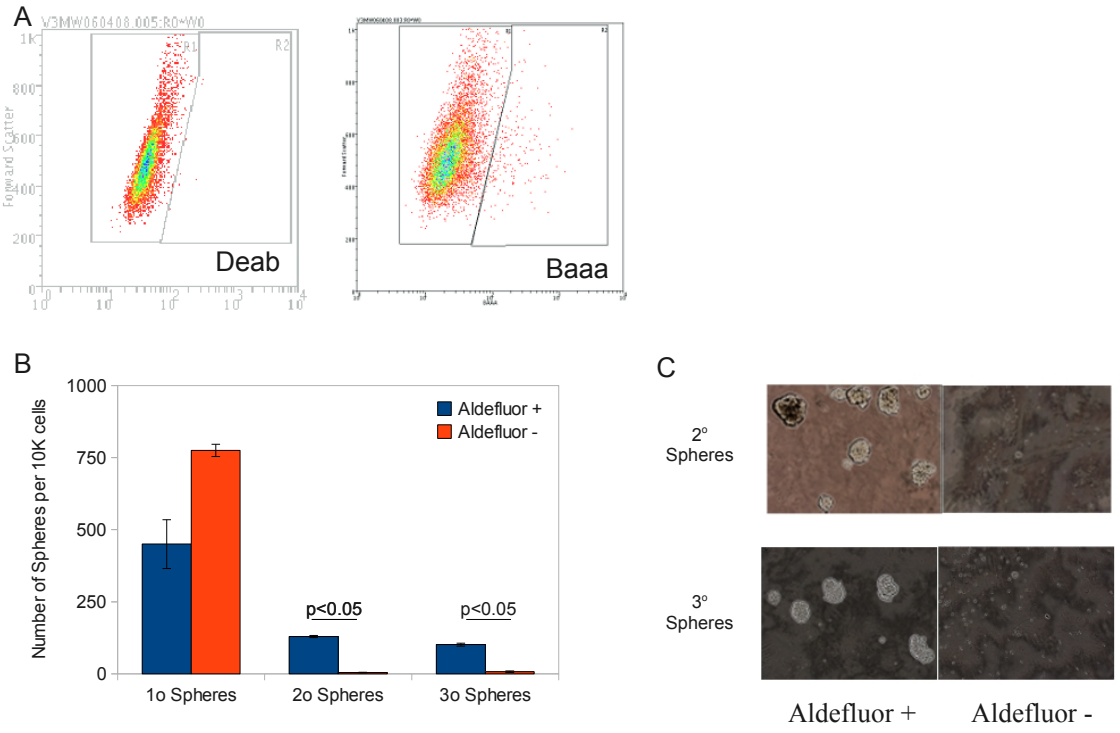

Figure 4.2. ALDH activity in a minority of human FTC cells. Human FTC cells from FTC236 or FTC238 were removed from culture and incubated with Baaa fluorescent substrate with or without ALDH inhibitor Deab. Baaa fluorescent substrate is freely diffusible until cleaved by ALDH.Channel protein inhibitor verapamil was also added to all samples to prevent dye efflux. Flow cytometric analysis of cells incubated with baaa and deab established the basal fluorescence levels without ALDH activity. Without DEAB, cells with high ALDH activity distinguished themselves with fluorescence level above the Deab treated cells. (B) Increased sphere-forming capacity by Aldefluor bright ($Aldf^{br)}$ cells. Cells were sorted by their Aldefluor status. Cells were placed in suspension culture in serum free media supplemented with EGF, bFGF, heparin, and B27 cocktail. Density was 10,000 cells per mL. After 7 days spheres larger than 40 microns were collected, counted, dissociated, and recultured. Aldefluor+ cells continued forming large spheres into their second and third passages while sphere formation for Aldefluor- cells quickly diminished.(C) Secondary and tertiary spheres in culture. Cells from dissociated spheres were collected and replaced in new serum-free suspension culture as before.

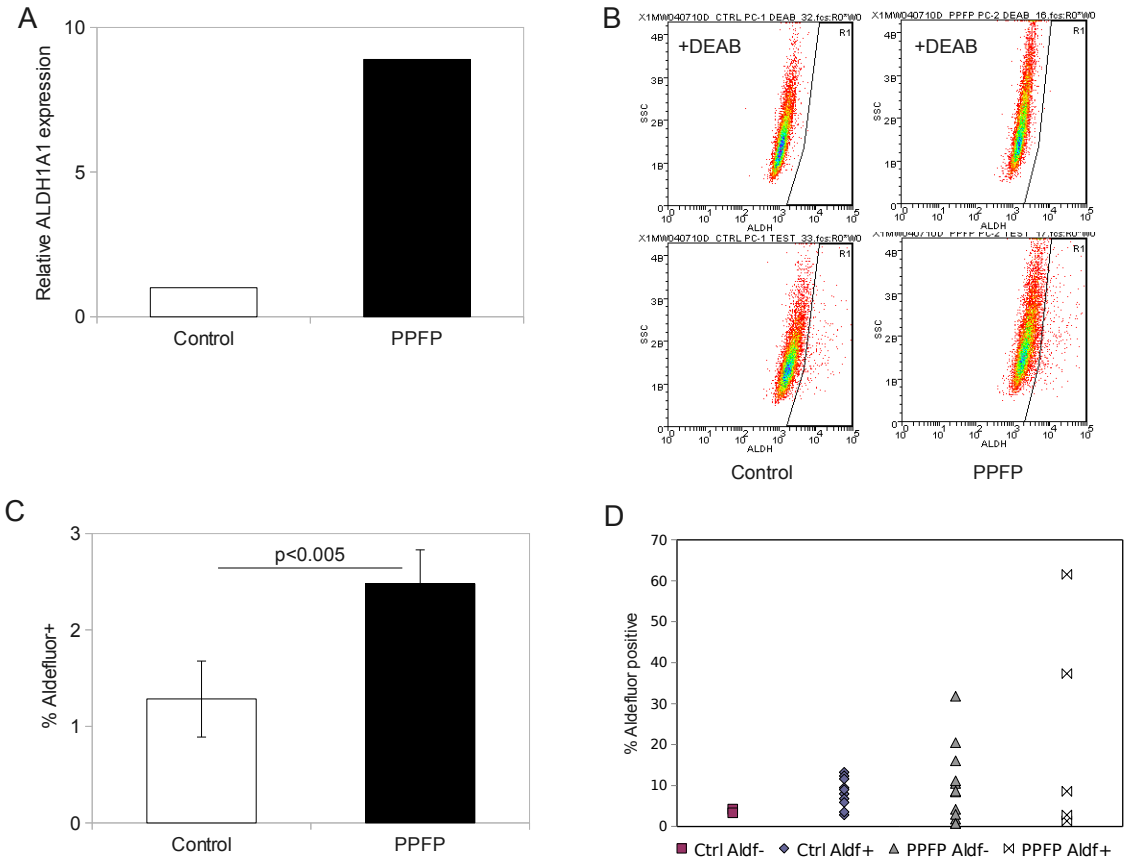

Figure 4.3. (A) Increased ALDH1A1 with PPFP expression. Empty vector control and PCCL3_PPFP were removed from culture and lysed with RealTime Ready Lysis Buffer. cDNA was synthesized from lysate with Transcriptor Universal cDNA Master. Real-time PCR was performed on a Lightcycler 480 using primers and probes from Roche's Universal Probe Library. Results were typical of repeated experiments. (B) Increased Aldefluor subpopulation with PPFP expression. Empty vector control and PCCL3_PPFP cells were removed from culture and prepared for Aldefluor analysis as previously described. Gates shown were set for the Deab control of each cell line; cells within the gate contained more GFP fluorescence than 99.9% of Deab treated control cells. (C) Quantitation of Aldefluor data. Control and PPFP cells were analysed for ALDH activity with the Aldefluor assay as described previously. Results shown are means ± SD and were typical of experiments using independent cell lines. (D) Aldefluor analysis of clones derived from single sorted cells. A single cell was sorted by its Aldefluor status into each well on a 96 well plates. Cells which grew into robust, passageable clonal cell lines were kept for analysis. Cell lines derived from Aldefluor dim cells were as capable of regenerating the Aldefluor heterogeneity of the parental population as cell lines derived from Aldefluor bright cells.

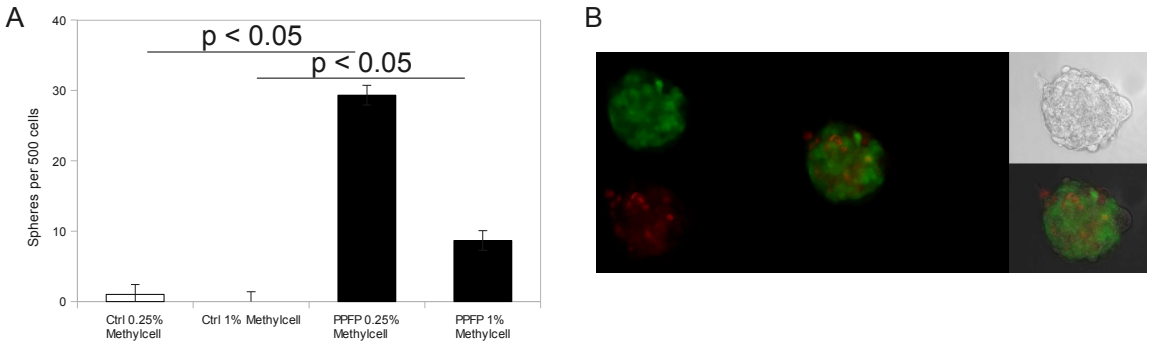

Figure 4.4. (A) Increased sphere formation by PPFP cells. PCCL3_PPFP and empty vector control cells were placed in serum free, suspension culture at 500 cells/ml density. Methyl cellulose was added to increase the media viscosity and prevent aggregation. PPFP cells formed many more spheres in culture than Control cells. The number of spheres declined as more methyl cellulose was added, suggesting that aggregation played a role in sphere formation. (B) PCCL3 spheres came from 2 or more cells. Equal number of DsRed and GFP cells were co-cultured and 80% of spheres contained a mosaic of both colors. A typical sphere was photographed and shown. In columns from left to right: GFP and DsRed channels separately; GFP and DsRed combined; phase contrast micrography by itself and combined with fluorescence micrography.

CHAPTER 5

Akt activation did not mediate TCF/Wnt activation in PPFP cells

Our lab found increased and heterogeneous phosphorylated Akt levels in a transgenic mouse model of PPFP expressing thyroid carcinoma (124). PPFP expressing PCCL3 cells contained a larger sub population of cells positive for phosphorylated Akt than control cells [Fig. 5.1A]. Akt regulates the Wnt/β-catenin/TCF pathway by phosphorylating GSK3β as well as β-catenin (67; 132). As such, Akt was a suspect in our search for mediators of PPFP-induced TCF activation.

However, inhibition of Akt, which effected lower phosphorylated active Akt in our cells, had no effect on TCF activation level. Treatment of PCCL3_PPFP and empty vector control cells with Akt inhibitor perifosine (up to 5μM) failed to diminish TCF_GFP+ cell numbers [Fig. 5.1B, C]. At 10μM, perifosine caused widespread cell death [data not shown]. We were concerned that at 5μM, perifosine may not be effective at inhibiting Akt. However, treatment with 5μM perifosine was sufficient to decrease levels of active Akt (phosphorylated at Ser473) by 60% [Fig. 5.1D].

That Wnt/TCF activation in PCCL3 cells did not require active Akt signalling was evident when we examined pAkt and TCF_GFP positivity concurrently. Despite high percentages of TCF_GFP+ and pAkt+ cells [Fig. 5.2A, B], only 0.5% of the population were positive for both [Fig. 5.2C]. Among TCF_GFP+ cells, pAkt+ cells comprised approximately the same percentage as in the whole population. Likewise among pAkt+ cells, TCF_GFP+ cells were not enriched for compared to the whole population.[Fig. 5.2D]

More direct manipulation of the Wnt/TCF pathway by the GSK-3β inhibitor BioIX increased TCF-responsive GFP transcription in our cell lines [Fig. 5.3].

These data suggested that activation of Akt found in PPFP FTC did not effect TCF activation.

Materials and Methods

Reagents

Perifosine was obtained from Keryx Biopharmaceuticals. Bio IX GSK-3β inhibitor and MeBio control were purchased from Milipore.

Flow Cytometry

Cells were removed from culture by trypsinization and fixed in 1.5% paraformaldehyde

for 30 minutes at room temperature. They were then permeabilized and stored in ice cold Methanol. Fixed cells were resuspended in HBBS, filtered through 40 micron sieve to discard aggregates, and incubated with anti-phosphoAkt (Ser473) antibody from Cell Signaling Technologies, diluted 1:250 in HBSS + 2% FBS. After washing in HBSS, cells were incubated with an APC conjugated anti-rabbit secondary antibody from Jackson Labs, diluted 1:250 in HBSS + 2% FBS. Cells were finally resuspended in HBSS + PI or DAPI and analyzed on a flow cytometer.

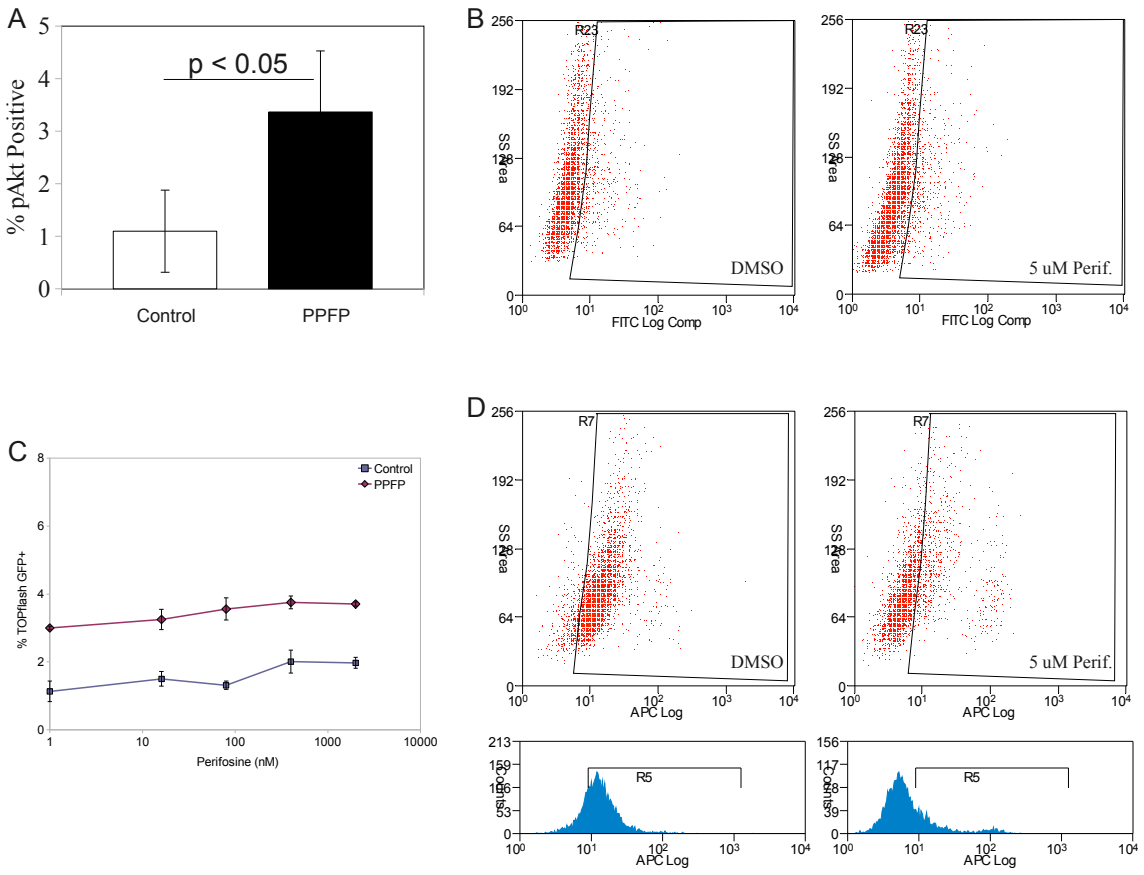

Figure 5.1. (A) Increased Akt activation in PPFP cells. PCCL3 cells were fixed with paraformaldehyde, permabilized with MeOH,and incubated with an antibody against Akt phosphorylated at Ser473 (i.e. active Akt). The primary antibody was recognized by a APC conjugated secondary antibody. Samples were analyzed via flow cytometry. Samples incubated without primary antibodies served as negative control and were used to set the gates. PCCL3_PPFP cells contained more cells with active pAkt than empty vector control. (B) PCCL3_PPFP cells expressing GFP under a TCF responsive promoter were treated with the Akt inhibitor Perifosine for 5 days then analyzed via flow cytometry. Gates were set using PCCL3 expressing GFP under a MCMV promoter. Perifosine treated cells contained the same percentage of cells with TCF_GFP positivity as vehicle treated control. (C) No effect of Akt inhibitor on TCF activation. Empty vector control and PCCL3_PPFP cells were treated with perifosine for 5 days. Cells were then removed from culture and analyzed via flow cytometry. Results are means ± SD. (D) Inhibition of active Akt by perifosine. Cells were treated with 5μM perifosine or vehicle for 5 days. They were then removed from culture, fixed and stained for pAkt as described before. Flow cytometry analysis demonstrated that treatment with perifosine caused a substantial decrease in signal levels as well as percentage of cells positive for pAkt.

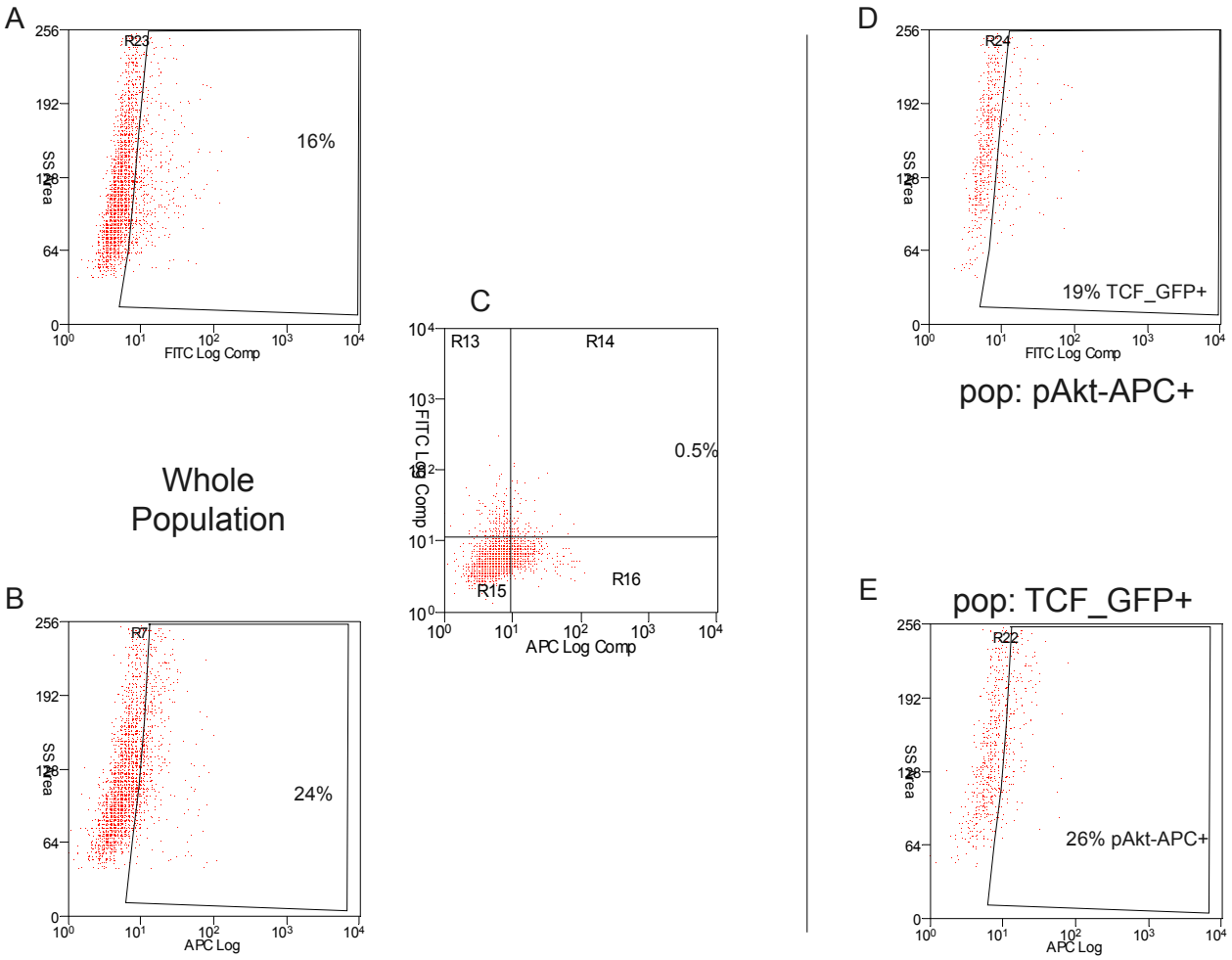

Figure 5.2. (A) Non-concurrent activation of Akt and TCF. PCCL3_PPFP expressing GFP under a TCF responsive promoter were fixed and stained for pAkt as described previously. The fixing protocol preserving GFP fluorescence. (B) Flow cytometry analysis of pAkt levels in PCCL3_PPFP cells. (C) Cells fixed to preserve GFP fluorescence and stained for pAkt contained only 0.5% double positive cells despite strong positivity for each color. (D) TCF activation in the pAkt positive population. Analysis of the pAkt-APC+ fraction revealed 19% GFP positivity compared to 16% in the whole population. (E) pAkt positivity in TCF_GFP+ population. Analysis of the GFP+ fraction revealed 26% pAkt-APC positivity compared to 24% in the whole population. Results are typical of multiple independent cell lines.

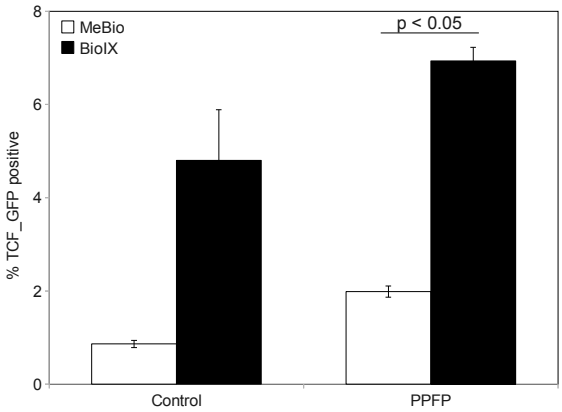

Figure 5.3. Increased TCF activation after GSK3β inhibition. PCCL3_PPFP and empty vector control cells were treated with the GSK3β inhibitor BioIX (1μM) for five days. Cells were then trypsinized and analyzed via flow cytometry for TCF driven GFP expression. Depicted are percent of cells with GFP levels higher than 99.5% of cells expressing GFP under MCMV promoter without TCF response elements. Results are means ± SD.

CHAPTER 6

DISCUSSION

We demonstrated that PPFP expression increased the percentage of cancer-stem-cell-like TCF responsive cells in PCCL3 cell lines, and that this increase was subject to manipulation via the PPARγ domains of PPFP. The TCF-responsive reporter systems may prove to be a powerful new way to isolate and study thyroid stem cells and cancer stem cells, while providing further insights on how the Wnt/TCF pathway regulates thyroid biology. The mechanism of PPFP transformation remains unclear. We demonstrated that the PPARγ domains of PPFP were essential. Modulations of those PPARγ domains will guide our future experiments to discover targets of PPFP transformation.

Activation of the Wnt/β-catenin/TCF pathway is well known in anaplastic and papillary thyroid carcinomas and has also been observed in follicular thyroid carcinomas. Nuclear localization of β-catenin is prevalent in the aforementioned cancers but is not common in normal thyroid tissues or thyroid adenomas (60; 61; 83; 127). Nonetheless, components of the Wnt pathways regulate thyrocyte proliferation and differentiated gene expression (133–135). Furthermore, the Wnt pathway plays an important role in development and

fate specification of the endoderm, the embryonic origin of the thyroid (136; 137). Wnt remains an important regulator of adult tissue stem cells in other endoderm derived tissues and its dysregulation causes cancers in those tissues (138). We suspect that the Wnt pathway is important to normal thyroid tissues and differentiated thyroid carcinomas even when activation of β-catenin is below the limit of detection.

GFP based TCF reporter systems and flow cytometric analysis allowed us to analyze large numbers of cells and detect even a small minority of TCF activated cells. We found 1-5% TCF responsive cells in empty vector control PCCL3 cell lines and 2 to 6 fold more in PCCL3_PPFP lines. These TCF responsive cells had the properties of cancer stem cells in vitro assays. We were unable to show enrichment of tumorigenicity in a particular sub-population since any small number of PCCL3 cells formed tumors in NOD_SCID mice without discrimination. The tumors were slow growing and did not reach experiment end-points until 6 to 8 months after injection. For this reason we would consider injecting tumor cells directly into the thyroid in future studies. While technically more difficult, the placement of cells into the appropriate microenvironment may allow a CSC fraction to demonstrate its proliferative advantage.

Some labs have also found broad tumorigenicity in different sub populations when using cell lines (47), while others found exclusive tumorigenicity in the cancer stem cell fraction when implanting primary human tumors in NOD_SCID mice (54).

Our PPFP^{+}/PTEN$^{thy-/-}$ mouse model of FTC gives us a unique opportunity to study tumorigenicity of different cell fractions using primary tumor tissues and challenging them to form tumors in syngeneic, immune competent mice. Our preliminary data showed that dissociated PPFP+/PTEN$^{thy-/-}$ primary tumors and metastases formed subcutaneous tumors when implanted in background strain mice. These tumors were recovered and serially passaged (i.e. injected into another mouse). Transfection of these tumor cells with a constitutive fluorescent marker would allow us to recover the injected cells from tumors while discarding host cells. Tumor formation, passageability, and specific recoverability are necessary characteristics needed for an assay of self renewal and tumorigenic capacity - i.e. an *in vivo* assay for cancer stem cells.

Our preliminary *in vitro* analyses of cells derived from PPFP^{+}/PTEN$^{thy-/-}$ tumors reproduced the hierarchy based on TCF responsiveness found in PCCL3 cells. We are eager to test the hypothesis that the TCF responsive sub population is enriched for self-renewing, tumorigenic cells in an immune competent syngeneic tumor model. Other previously published thyroid cancer stem cell markers can also be tested in this manner, including aldehyde dehydrogenase activity which successfully isolated xenograft-forming human thyroid cancer stem cells (54). Our preliminary data showed that ALDH gene expression and activity were elevated by PPFP expression, but the regenerative potential was not as strictly segregated in the Aldefluor hierarchy as it was in the TCF hierarchy.

The significance of TCF activation and its relationship to PPFP are unclear beyond our

demonstration that cells which effect the phenotypes of PPFP driven transformation are derived from TCF-responsive cells. The size of the TCF responsive fraction did not correlate to invasive capacity in our study of PCCL3_PPFP clones. Pioglitazone induced a slight increase in TCF responsive cells in our clones derived from GFP negative cells, but a disproportionately larger increase in invasive capacity. Aside from incidental observations that PPARγ antagonists decreased TCF_GFP positivity, our efforts to disrupt TCF activation have so far yielded negative results. Therefore we are still not certain if TCF activation is an essential part of PPFP transformation or merely indicative of PPFP actions on other pathways which resulted in increased self-renewal and enlargement of the TCF responsive cancer stem cells sub population.

There are 4 members in the Lef/Tcf family which form complexes with β-catenin and express canonical Wnt target genes. TCF7L2/TCF4 is present in PTC and implicated in transcription of Wnt/β-catenin target genes (139). TCF7L2 was upregulated in PCCL3_PPFP cells, but our targeting of TCF7L2 did not impact TCF_GFP positivity. It is possible that more than 1 member of the Lef/Tcf family are active in the thyroid, have redundant functions, and must be knocked down in combination before TCF responsive transcription is impacted.

Our data showed that the PPARγ domains of PPFP retained their ability to act in a PPARγ-like manner and transactivate PPARγ target genes. The PPARγ DNA binding domain is required for PPFP functions. Same with PPARγ ligand binding domain: PPARγ

agonists increased the effects of PPFP in a PPARγ specific manner. PPARγ selective agonists which can activate certain PPARγ transcriptional programs but not others also strengthened the effects of PPFP.

We would predict that selective PPARγ agonists would not be useful for treating PPFP positive FTC. We previously reported the potent anti-tumor and adipogenic transdifferentiating effect of pioglitazone (39). Pioglitazone is clinically useful against diabetes, but its many side effects motivated research into selective PPARγ agonists which could effect the insulin sensitization of full agonists without the adipogenesis associated side effects. We demonstrated that a non-adipogenic selective agonist had no anti-tumor effect *in vivo*. Our *in vitro* data further implied that a non-adipogenic selective agonist would instead exacerbate PPFP oncogenesis by increasing the number of cancer stem cells.

Other clues for the mechanism of PPFP oncogenesis could continue to come from diabetes-focused research into selective PPARγ agonists. Selective PPARγ agonists block Cdk5 phosphorylation of PPARγ and this is sufficient to produce known effects of PPARγ without full allosteric agonism (109; 123). Dysregulation of Cdk5 or inaccessibility of the Cdk5 phosphorylation site on PPFP may play a role in PPFP action. Determining the basal level of PPFP phosphorylation at the Cdk5 phosphorylation site and whether any agonist induced changes occurred would tell us whether Cdk5 regulation of PPFP is likely relevant to oncogenesis.

Another proposed mechanism of selective PPARγ agonist action is differential recruitment of coactivators. PPARγ transactivation requires recruitment of coactivators. The large number of coactivators and their variable expression determine the cell-specific PPARγ transcriptional program. selective PPARγ agonists preferentially recruit certain co-activators compared to the classical agonists. PPARγ coactivator 1 α (PGC1α) is preferentially recruited by 3 distinct selective agonists (140–142). Targeting PGC1α would reveal whether it is required for PPFP oncogenesis, while co-IP would reveal whether it is indeed in complex with PPFP. Other coactivators - cAMP response element-binding protein-binding protein and steroid receptor coactivator-1 - are more weakly recruited or prevented from complexing by multiple selective agonists (140; 142–144). Manipulations of these proteins are less likely to be informative - overexpression or knock down of these proteins would be ineffective if there's little or no interaction. We remain mindful that nuclear receptors can have non-transcriptional effects (145) and putative non-transcriptional actions of PPARγ may turn out relevant to PPFP oncogenesis.

The effects of full and selective PPARγ agonists on PPFP and the necessity of a functional PPARγ DNA binding domain also suggested a new strategy to discover targets of PPFP. If PPFP has its own oncogenic transcriptional program (or simply a set of PPFP bound genes), direct transcriptional targets of PPFP are discoverable through chromatin IP and high throughput sequencing (ChIP-SEQ). The results would be another test of our

hypothesis that PPFP binds PPARγ target genes and response elements. Novel consensus elements recognized by PPFP may also be uncovered, along with new target genes. The list of interesting targets to be investigated may be narrowed down to those genes that are further enriched after treatment with PPARγ agonist pioglitazone and selective agonist SR1664.

Finally, our collection of PCCL3_PPFP and PPFP+/PTEN-/- clones is an important resource for investigating and validating targets suspected to impact cancer stem cells. Changes in the cancer stem cell fraction are masked by the biology of the bulk population. Cell sorting enriches for cancer stem cells but is time and resource intensive. Our population of clones includes entirely TCF unresponsive populations as well as populations containing a wide range of TCF responsive fractions. The clones also exhibit a wide range of colony formation and invasive capacity. Examination of differences between these populations may reveal the regulators of self-renewal and oncogenesis.

BIBLIOGRAPHY

1. Arufe MC, Lu M, Kubo A, Keller G, Davies TF, Lin R-Y. Directed differentiation of mouse embryonic stem cells into thyroid follicular cells. Endocrinology 2006 Jun;147(6):3007–3015.[cited 2012 Jul 3]

2. Lin R-Y, Kubo A, Keller GM, Davies TF. Committing Embryonic Stem Cells to Differentiate into Thyrocyte-Like Cells in Vitro. Endocrinology 2003 Jun;144(6):2644–2649.[cited 2012 Jul 1]

3. Jiang N, Hu Y, Liu X, Wu Y, Zhang H, Chen G, Liang J, Lu X, Liu S. Differentiation of E14 mouse embryonic stem cells into thyrocytes in vitro. Thyroid 2010 Jan;20(1):77–84.[cited 2012 Jul 3]

4. Chebath J, Chabaud O, Mauchamp J. Modulation of thyroglobulin messenger RNA level by thyrotropin in cultured thyroid cells. Nucleic Acids Res. 1979 Jul;6(10):3353–3367.

5. Heuverswyn BV, Streydio C, Brocas H, Refetoff S, Dumont J, Vassart G. Thyrotropin controls transcription of the thyroglobulin gene. PNAS 1984 Oct;81(19):5941–5945.[cited 2012 Oct 3]

6. Kogai T, Endo T, Saito T, Miyazaki A, Kawaguchi A, Onaya T. Regulation by Thyroid-Stimulating Hormone of Sodium/Iodide Symporter Gene Expression and Protein Levels in FRTL-5 Cells. Endocrinology 1997 Jun;138(6):2227–2232.[cited 2012 Oct 3]

7. Mascia A, Nitsch L, Lauro RD, Zannini M. Hormonal control of the transcription factor Pax8 and its role in the regulation of thyroglobulin gene expression in thyroid cells. J Endocrinol 2002 Jan;172(1):163–176.[cited 2012 Oct 3]

8. Kimura T, Keymeulen AV, Golstein J, Fusco A, Dumont JE, Roger PP. Regulation of Thyroid Cell Proliferation by TSH and Other Factors: A Critical Evaluation of in Vitro Models. Endocrine Reviews 2001 Oct;22(5):631–656.[cited 2012 Oct 3]

9. Chiamolera MI, Wondisford FE. Thyrotropin-Releasing Hormone and the Thyroid Hormone Feedback Mechanism. Endocrinology 2009 Mar;150(3):1091–1096.[cited 2012 Oct 3]

10. Suzuki K, Kawashima A, Yoshihara A, Akama T, Sue M, Yoshida A, Kimura HJ. Role of thyroglobulin on negative feedback autoregulation of thyroid follicular function and growth. Journal of Endocrinology 2011 Mar;209(2):169–174.[cited 2012 Sep 25]

11. Felice MD, Postiglione MP, Lauro RD. Minireview: Thyrotropin Receptor Signaling in Development and Differentiation of the Thyroid Gland: Insights from Mouse Models and Human Diseases. Endocrinology 2004 Sep;145(9):4062–4067.[cited 2012 Oct 3]

12. Takahashi S, Conti M, Prokop C, Van Wyk JJ, Earp HS 3rd. Thyrotropin and insulin-like growth factor I regulation of tyrosine phosphorylation in FRTL-5 cells. Interaction between cAMP-dependent and growth factor-dependent signal transduction. J. Biol. Chem. 1991 Apr;266(12):7834–7841.

13. Van Keymeulen A, Dumont JE, Roger PP. TSH induces insulin receptors that mediate insulin costimulation of growth in normal human thyroid cells. Biochem. Biophys. Res. Commun. 2000 Dec;279(1):202–207.

14. Fierabracci A, Puglisi MA, Giuliani L, Mattarocci S, Gallinella-Muzi M. Identification of an adult stem/progenitor cell-like population in the human thyroid. J Endocrinol 2008 Sep;198(3):471–487.[cited 2012 Jul 10]

15. Lan L, Cui D, Nowka K, Derwahl M. Stem Cells Derived from Goiters in Adults Form Spheres in Response to Intense Growth Stimulation and Require Thyrotropin for Differentiation into Thyrocytes. J Clin Endocrinol Metab 2007 Sep;92(9):3681–3688.[cited 2010 Aug 3]

16. Cancer of the Thyroid - SEER Stat Fact Sheets [Internet]. [date unknown];[cited 2012 Oct 4] Available from: http://seer.cancer.gov/statfacts/html/thyro.html

17. Tuttle RM, Ball DW, Byrd D, Dilawari RA, Doherty GM, Duh Q-Y, Ehya H, Farrar WB, Haddad RI, Kandeel F, Kloos RT, Kopp P, Lamonica DM, Loree TR, Lydiatt WM, McCaffrey JC, Olson JA, Parks L, Ridge JA, Shah JP, Sherman SI, Sturgeon C, Waguespack SG, Wang TN, Wirth LJ. Thyroid Carcinoma. J Natl Compr Canc Netw 2010 Nov;8(11):1228–1274.[cited 2012 Sep 26]

18. Cooper DS, Doherty GM, Haugen BR, Kloos RT, Lee SL, Mandel SJ, Mazzaferri EL, McIver B, Pacini F, Schlumberger M, Sherman SI, Steward DL, Tuttle RM. Revised American Thyroid Association Management Guidelines for Patients with Thyroid Nodules and Differentiated Thyroid Cancer. Thyroid 2009 Nov;19(11):1167–1214.[cited 2012 Oct 2]

19. Baloch ZW, LiVolsi VA. Pathologic diagnosis of papillary thyroid carcinoma: today and tomorrow. Expert Review of Molecular Diagnostics 2005 Jul;5(4):573+.

20. Sobrinho-Simões M, Eloy C, Magalhães J, Lobo C, Amaro T. Follicular thyroid carcinoma. Modern Pathology 2011;24:S10–S18.[cited 2012 Oct 4]

21. Ruegemer JJ, Hay ID, Bergstralh EJ, Ryan JJ, Offord KP, Gorman CA. Distant Metastases in Differentiated Thyroid Carcinoma: A Multivariate Analysis of

Prognostic Variables. JCEM 1988 Sep;67(3):501–508.[cited 2012 Oct 4]

22. Bhaijee F, Nikiforov Y. Molecular Analysis of Thyroid Tumors. Endocrine Pathology 2011;22(3):126–133.[cited 2012 Sep 26]

23. Giordano TJ, Kuick R, Thomas DG, Misek DE, Vinco M, Sanders D, Zhu Z, Ciampi R, Roh M, Shedden K, others. Molecular classification of papillary thyroid carcinoma: distinct BRAF, RAS, and RET/PTC mutation-specific gene expression profiles discovered by DNA microarray analysis. Oncogene 2005;24(44):6646–6656.

24. Giordano TJ, Au AYM, Kuick R, Thomas DG, Rhodes DR, Wilhelm KG, Vinco M, Misek DE, Sanders D, Zhu Z, Ciampi R, Hanash S, Chinnaiyan A, Clifton-Bligh RJ, Robinson BG, Nikiforov YE, Koenig RJ. Delineation, Functional Validation, and Bioinformatic Evaluation of Gene Expression in Thyroid Follicular Carcinomas with the PAX8-PPARG Translocation. Clinical Cancer Research 2006 Apr;12(7):1983–1993.[cited 2010 Jun 13]

25. Nikiforova MN, Lynch RA, Biddinger PW, Alexander EK, Dorn GW, Tallini G, Kroll TG, Nikiforov YE. RAS Point Mutations and PAX8-PPARγ Rearrangement in Thyroid Tumors: Evidence for Distinct Molecular Pathways in Thyroid Follicular Carcinoma. JCEM 2003 May;88(5):2318–2326.[cited 2012 Jul 10]

26. Banito A, Pinto AE, Espadinha C, Marques AR, Leite V. Aneuploidy and RAS mutations are mutually exclusive events in the development of well-differentiated thyroid follicular tumours. Clinical Endocrinology 2007;67(5):706–711.[cited 2012 Jun 30]

27. Druker BJ, Lydon NB. Lessons learned from the development of an Abl tyrosine kinase inhibitor for chronic myelogenous leukemia. Journal of Clinical Investigation 2000 Jan;105(1):3–7.[cited 2012 Oct 4]

28. Lynch TJ, Bell DW, Sordella R, Gurubhagavatula S, Okimoto RA, Brannigan BW, Harris PL, Haserlat SM, Supko JG, Haluska FG, Louis DN, Christiani DC, Settleman J, Haber DA. Activating mutations in the epidermal growth factor receptor underlying responsiveness of non-small-cell lung cancer to gefitinib. N. Engl. J. Med. 2004 May;350(21):2129–2139.

29. Pegram MD, Lipton A, Hayes DF, Weber BL, Baselga JM, Tripathy D, Baly D, Baughman SA, Twaddell T, Glaspy JA, Slamon DJ. Phase II study of receptor-enhanced chemosensitivity using recombinant humanized anti-p185HER2/neu monoclonal antibody plus cisplatin in patients with HER2/neu-overexpressing metastatic breast cancer refractory to chemotherapy treatment. J. Clin. Oncol. 1998 Aug;16(8):2659–2671.

30. Slamon DJ, Leyland-Jones B, Shak S, Fuchs H, Paton V, Bajamonde A, Fleming T,

Eiermann W, Wolter J, Pegram M, Baselga J, Norton L. Use of chemotherapy plus a monoclonal antibody against HER2 for metastatic breast cancer that overexpresses HER2. N. Engl. J. Med. 2001 Mar;344(11):783–792.

31. Vogel CL, Cobleigh MA, Tripathy D, Gutheil JC, Harris LN, Fehrenbacher L, Slamon DJ, Murphy M, Novotny WF, Burchmore M, Shak S, Stewart SJ, Press M. Efficacy and Safety of Trastuzumab as a Single Agent in First-Line Treatment of HER2-Overexpressing Metastatic Breast Cancer. JCO 2002 Feb;20(3):719–726. [cited 2012 Oct 4]

32. Pérez-Soler R, Chachoua A, Hammond LA, Rowinsky EK, Huberman M, Karp D, Rigas J, Clark GM, Santabárbara P, Bonomi P. Determinants of tumor response and survival with erlotinib in patients with non--small-cell lung cancer. J. Clin. Oncol. 2004 Aug;22(16):3238–3247.

33. Lynch TJ, Bell DW, Sordella R, Gurubhagavatula S, Okimoto RA, Brannigan BW, Harris PL, Haserlat SM, Supko JG, Haluska FG, Louis DN, Christiani DC, Settleman J, Haber DA. Activating mutations in the epidermal growth factor receptor underlying responsiveness of non-small-cell lung cancer to gefitinib. N. Engl. J. Med. 2004 May;350(21):2129–2139.

34. Sherman SI. Targeted therapies for thyroid tumors. Modern Pathology 2011;24:S44–S52.[cited 2012 Sep 26]

35. Thornton K, Kim G, Maher VE, Chattopadhyay S, Tang S, Moon YJ, Song P, Marathe A, Balakrishnan S, Zhu H, Garnett C, Liu Q, Booth B, Gehrke B, Dorsam R, Verbois L, Ghosh D, Wilson W, Duan J, Sarker H, Miksinski SP, Skarupa L, Ibrahim A, Justice R, Murgo A, Pazdur R. Vandetanib for the treatment of symptomatic or progressive medullary thyroid cancer in patients with unresectable locally advanced or metastatic disease: U.S. Food and Drug Administration drug approval summary. Clin. Cancer Res. 2012 Jul;18(14):3722–3730.

36. Leboulleux S, Bastholt L, Krause T, De la Fouchardiere C, Tennvall J, Awada A, Gómez JM, Bonichon F, Leenhardt L, Soufflet C, Licour M, Schlumberger MJ. Vandetanib in locally advanced or metastatic differentiated thyroid cancer: a randomised, double-blind, phase 2 trial. Lancet Oncol. 2012 Sep;13(9):897–905.

37. Kurzrock R, Sherman SI, Ball DW, Forastiere AA, Cohen RB, Mehra R, Pfister DG, Cohen EEW, Janisch L, Nauling F, Hong DS, Ng CS, Ye L, Gagel RF, Frye J, Müller T, Ratain MJ, Salgia R. Activity of XL184 (Cabozantinib), an oral tyrosine kinase inhibitor, in patients with medullary thyroid cancer. J. Clin. Oncol. 2011 Jul;29(19):2660–2666.

38. An international, double-blind, randomized, placebo-controlled phase III trial (EXAM) of cabozantinib (XL184) in medullary thyroid carcinoma (MTC) patients

(pts) with documented RECIST progression at baseline. - ASCO [Internet]. [date unknown];[cited 2012 Oct 5] Available from: http://www.asco.org/ASCOv2/Meetings/Abstracts?&vmview=abst_detail_view&confID=114&abstractID=94113

39. Dobson ME, Diallo-Krou E, Grachtchouk V, Yu J, Colby LA, Wilkinson JE, Giordano TJ, Koenig RJ. Pioglitazone Induces a Proadipogenic Antitumor Response in Mice with PAX8-PPARγ Fusion Protein Thyroid Carcinoma. Endocrinology 2011 Nov;152(11):4455–4465.[cited 2012 Jul 3]

40. Zheng X, Cui D, Xu S, Brabant G, Derwahl M. Doxorubicin fails to eradicate cancer stem cells derived from anaplastic thyroid carcinoma cells: characterization of resistant cells. Int. J. Oncol. 2010 Aug;37(2):307–315.[cited 2012 Jul 3]

41. Dick JE. Stem cell concepts renew cancer research. Blood 2008 Dec;112(13):4793–4807.[cited 2012 Oct 5]

42. Hoshi N, Kusakabe T, Taylor BJ, Kimura S. Side Population Cells in the Mouse Thyroid Exhibit Stem/Progenitor Cell-Like Characteristics. Endocrinology 2007 Sep;148(9):4251–4258.[cited 2012 Jul 1]

43. Mitsutake N, Iwao A, Nagai K, Namba H, Ohtsuru A, Saenko V, Yamashita S. Characterization of side population in thyroid cancer cell lines: cancer stem-like cells are enriched partly but not exclusively. Endocrinology 2007 Apr;148(4):1797–1803.[cited 2012 Jul 3]

44. Zito G, Richiusa P, Bommarito A, Carissimi E, Russo L, Coppola A, Zerilli M, Rodolico V, Criscimanna A, Amato M, Pizzolanti G, Galluzzo A, Giordano C. In Vitro Identification and Characterization of CD133pos Cancer Stem-Like Cells in Anaplastic Thyroid Carcinoma Cell Lines. PLoS ONE [date unknown];3(10)

45. Zhu W, Hai T, Ye L, Cote GJ. Medullary Thyroid Carcinoma Cell Lines Contain a Self-Renewing CD133+ Population that Is Dependent on Ret Proto-Oncogene Activity. J Clin Endocrinol Metab 2010 Jan;95(1):439–444.[cited 2010 Aug 3]

46. Liu J, Brown RE. Immunohistochemical detection of epithelialmesenchymal transition associated with stemness phenotype in anaplastic thyroid carcinoma. Int J Clin Exp Pathol 2010;3(8):755–762.[cited 2012 Jul 3]

47. Friedman S, Lu M, Schultz A, Thomas D, Lin R-Y. CD133+ anaplastic thyroid cancer cells initiate tumors in immunodeficient mice and are regulated by thyrotropin. PLoS ONE 2009;4(4):e5395.[cited 2012 Jul 3]

48. Tseng L-M, Huang P-I, Chen Y-R, Chen Y-C, Chou Y-C, Chen Y-W, Chang Y-L, Hsu H-S, Lan Y-T, Chen K-H, Chi C-W, Chiou S-H, Yang D-M, Lee C-H. Targeting Signal Transducer and Activator of Transcription 3 Pathway by Cucurbitacin I

Diminishes Self-Renewing and Radiochemoresistant Abilities in Thyroid Cancer-Derived CD133+ Cells. J Pharmacol Exp Ther 2012 May;341(2):410–423.[cited 2012 Oct 5]

49. Kohn FR, Sladek NE. Aldehyde dehydrogenase activity as the basis for the relative insensitivity of murine pluripotent hematopoietic stem cells to oxazaphosphorines. Biochem. Pharmacol. 1985 Oct;34(19):3465–3471.

50. Chen M, Achkar C, Gudas LJ. Enzymatic conversion of retinaldehyde to retinoic acid by cloned murine cytosolic and mitochondrial aldehyde dehydrogenases. Mol. Pharmacol. 1994 Jul;46(1):88–96.

51. Storms RW, Trujillo AP, Springer JB, Shah L, Colvin OM, Ludeman SM, Smith C. Isolation of primitive human hematopoietic progenitors on the basis of aldehyde dehydrogenase activity. Proc. Natl. Acad. Sci. U.S.A. 1999 Aug;96(16):9118–9123.

52. Corti S, Locatelli F, Papadimitriou D, Donadoni C, Salani S, Del Bo R, Strazzer S, Bresolin N, Comi GP. Identification of a primitive brain-derived neural stem cell population based on aldehyde dehydrogenase activity. Stem Cells 2006 Apr;24(4):975–985.

53. Ginestier C, Hur MH, Charafe-Jauffret E, Monville F, Dutcher J, Brown M, Jacquemier J, Viens P, Kleer CG, Liu S, Schott A, Hayes D, Birnbaum D, Wicha MS, Dontu G. ALDH1 is a marker of normal and malignant human mammary stem cells and a predictor of poor clinical outcome. Cell Stem Cell 2007 Nov;1(5):555–567.

54. Todaro M, Iovino F, Eterno V, Cammareri P, Gambara G, Espina V, Gulotta G, Dieli F, Giordano S, De Maria R, Stassi G. Tumorigenic and Metastatic Activity of Human Thyroid Cancer Stem Cells. Cancer Research 2010 Nov;70(21):8874 –8885. [cited 2011 Jan 19]

55. Suzuki K, Mitsutake N, Saenko V, Suzuki M, Matsuse M, Ohtsuru A, Kumagai A, Uga T, Yano H, Nagayama Y, Yamashita S. Dedifferentiation of Human Primary Thyrocytes into Multilineage Progenitor Cells without Gene Introduction [Internet]. PLoS One 2011 Apr;6(4)[cited 2012 Oct 3] Available from: http://www.ncbi.nlm.nih.gov/pmc/articles/PMC3083435/

56. Chen G, Xu S, Renko K, Derwahl M. Metformin inhibits growth of thyroid carcinoma cells, suppresses self-renewal of derived cancer stem cells, and potentiates the effect of chemotherapeutic agents. J. Clin. Endocrinol. Metab. 2012 Apr;97(4):E510–520.[cited 2012 Jul 3]

57. Malaguarnera R, Frasca F, Garozzo A, Gianì F, Pandini G, Vella V, Vigneri R, Belfiore A. Insulin Receptor Isoforms and Insulin-Like Growth Factor Receptor in Human Follicular Cell Precursors from Papillary Thyroid Cancer and Normal

Thyroid. JCEM 2011 Mar;96(3):766–774.[cited 2012 Sep 26]

58. Zhang P, Zuo H, Ozaki T, Nakagomi N, Kakudo K. Cancer stem cell hypothesis in thyroid cancer. Pathology International 2006;56(9):485–489.[cited 2012 Sep 26]

59. Clevers H, Nusse R. Wnt/β-Catenin Signaling and Disease. Cell 2012 Jun;149(6):1192–1205.[cited 2012 Oct 10]

60. Garcia-Rostan G, Tallini G, Herrero A, D'Aquila TG, Carcangiu ML, Rimm DL. Frequent mutation and nuclear localization of beta-catenin in anaplastic thyroid carcinoma. Cancer Res. 1999 Apr;59(8):1811–1815.[cited 2012 Jul 10]

61. Garcia-Rostan G, Camp RL, Herrero A, Carcangiu ML, Rimm DL, Tallini G. β-Catenin Dysregulation in Thyroid Neoplasms. Am J Pathol 2001 Mar;158(3):987–996.

62. Kurihara T, Ikeda S, Ishizaki Y, Fujimori M, Tokumoto N, Hirata Y, Ozaki S, Okajima M, Sugino K, Asahara T. Immunohistochemical and sequencing analyses of the Wnt signaling components in Japanese anaplastic thyroid cancers. Thyroid 2004 Dec;14(12):1020–1029.[cited 2012 Jul 2]

63. Cetta F, Toti P, Petracci M, Montalto G, Disanto A, Lorè F, Fusco A. Thyroid carcinoma associated with familial adenomatous polyposis. Histopathology 1997 Sep;31(3):231–236.

64. Cetta F, Olschwang S, Petracci M, Montalto G, Baldi C, Zuckermann M, Mariani Costantini R, Fusco A. Genetic alterations in thyroid carcinoma associated with familial adenomatous polyposis: clinical implications and suggestions for early detection. World J Surg 1998 Dec;22(12):1231–1236.

65. Ishigaki K, Namba H, Nakashima M, Nakayama T, Mitsutake N, Hayashi T, Maeda S, Ichinose M, Kanematsu T, Yamashita S. Aberrant localization of beta-catenin correlates with overexpression of its target gene in human papillary thyroid cancer. J. Clin. Endocrinol. Metab. 2002 Jul;87(7):3433–3440.[cited 2012 Jul 2]

66. Rezk S, Brynes RK, Nelson V, Thein M, Patwardhan N, Fischer A, Khan A. beta-Catenin expression in thyroid follicular lesions: potential role in nuclear envelope changes in papillary carcinomas. Endocr. Pathol. 2004;15(4):329–337.[cited 2012 Jul 2]

67. Korkaya H, Paulson A, Charafe-Jauffret E, Ginestier C, Brown M, Dutcher J, Clouthier SG, Wicha MS. Regulation of Mammary Stem/Progenitor Cells by PTEN/Akt/β-Catenin Signaling. PLoS Biol 2009 Jun;7(6):e1000121.[cited 2010 Jun 3]

68. Bowers DC, Fan S, Walter KA, Abounader R, Williams JA, Rosen EM, Laterra J.

Scatter factor/hepatocyte growth factor protects against cytotoxic death in human glioblastoma via phosphatidylinositol 3-kinase- and AKT-dependent pathways. Cancer Res. 2000 Aug;60(15):4277–4283.

69. Xiao GH, Jeffers M, Bellacosa A, Mitsuuchi Y, Vande Woude GF, Testa JR. Anti-apoptotic signaling by hepatocyte growth factor/Met via the phosphatidylinositol 3-kinase/Akt and mitogen-activated protein kinase pathways. Proc. Natl. Acad. Sci. U.S.A. 2001 Jan;98(1):247–252.

70. Murakami H, Iwashita T, Asai N, Shimono Y, Iwata Y, Kawai K, Takahashi M. Enhanced phosphatidylinositol 3-kinase activity and high phosphorylation state of its downstream signalling molecules mediated by ret with the MEN 2B mutation. Biochem. Biophys. Res. Commun. 1999 Aug;262(1):68–75.

71. Cassinelli G, Favini E, Degl'Innocenti D, Salvi A, De Petro G, Pierotti MA, Zunino F, Borrello MG, Lanzi C. RET/PTC1-driven neoplastic transformation and proinvasive phenotype of human thyrocytes involve Met induction and beta-catenin nuclear translocation. Neoplasia 2009 Jan;11(1):10–21.[cited 2012 Jul 2]

72. Liaw D, Marsh DJ, Li J, Dahia PL, Wang SI, Zheng Z, Bose S, Call KM, Tsou HC, Peacocke M, Eng C, Parsons R. Germline mutations of the PTEN gene in Cowden disease, an inherited breast and thyroid cancer syndrome. Nat. Genet. 1997 May;16(1):64–67.

73. Stambolic V, Suzuki A, De la Pompa JL, Brothers GM, Mirtsos C, Sasaki T, Ruland J, Penninger JM, Siderovski DP, Mak TW. Negative regulation of PKB/Akt-dependent cell survival by the tumor suppressor PTEN. Cell 1998 Oct;95(1):29–39.

74. Cho NL, Lin C-I, Whang EE, Carothers AM, Moore FD Jr, Ruan DT. Sulindac reverses aberrant expression and localization of beta-catenin in papillary thyroid cancer cells with the BRAFV600E mutation. Thyroid 2010 Jun;20(6):615–622. [cited 2012 Jul 2]

75. Groden J, Thliveris A, Samowitz W, Carlson M, Gelbert L, Albertsen H, Joslyn G, Stevens J, Spirio L, Robertson M. Identification and characterization of the familial adenomatous polyposis coli gene. Cell 1991 Aug;66(3):589–600.

76. Korinek V, Barker N, Morin PJ, Wichen D van, Weger R de, Kinzler KW, Vogelstein B, Clevers H. Constitutive Transcriptional Activation by a β-Catenin-Tcf Complex in APC−/− Colon Carcinoma. Science 1997 Mar;275(5307):1784–1787.[cited 2012 Jul 6]

77. Korinek V, Barker N, Moerer P, Van Donselaar E, Huls G, Peters PJ, Clevers H. Depletion of epithelial stem-cell compartments in the small intestine of mice lacking Tcf-4. Nat. Genet. 1998 Aug;19(4):379–383.[cited 2012 Jul 6]

78. Barker N, Van Es JH, Kuipers J, Kujala P, Van den Born M, Cozijnsen M, Haegebarth A, Korving J, Begthel H, Peters PJ, Clevers H. Identification of stem cells in small intestine and colon by marker gene Lgr5. Nature 2007 Oct;449(7165):1003–1007.[cited 2012 Jul 6]

79. Barker N, Ridgway RA, Van Es JH, Van de Wetering M, Begthel H, Van den Born M, Danenberg E, Clarke AR, Sansom OJ, Clevers H. Crypt stem cells as the cells-of-origin of intestinal cancer. Nature 2009 Jan;457(7229):608–611.[cited 2012 Jul 6]

80. Kemper K, Prasetyanti PR, De Lau W, Rodermond H, Clevers H, Medema JP. Monoclonal Antibodies Against Lgr5 Identify Human Colorectal Cancer Stem Cells. Stem Cells 2012 Sep;

81. Schepers AG, Snippert HJ, Stange DE, Born M van den, Es JH van, Wetering M van de, Clevers H. Lineage Tracing Reveals Lgr5+ Stem Cell Activity in Mouse Intestinal Adenomas. Science 2012 Aug;337(6095):730–735.[cited 2012 Oct 5]

82. Vermeulen L, De Sousa E Melo F, Van der Heijden M, Cameron K, De Jong JH, Borovski T, Tuynman JB, Todaro M, Merz C, Rodermond H, Sprick MR, Kemper K, Richel DJ, Stassi G, Medema JP. Wnt activity defines colon cancer stem cells and is regulated by the microenvironment. Nat. Cell Biol. 2010 May;12(5):468–476. [cited 2012 Jul 6]

83. Helmbrecht K, Kispert A, Wasielewski R von, Brabant G. Identification of a Wnt/β-Catenin Signaling Pathway in Human Thyroid Cells. Endocrinology 2001 Dec;142(12):5261–5266.[cited 2012 Jul 10]

84. Castellone MD, De Falco V, Rao DM, Bellelli R, Muthu M, Basolo F, Fusco A, Gutkind JS, Santoro M. The {beta}-Catenin Axis Integrates Multiple Signals Downstream from RET/Papillary Thyroid Carcinoma Leading to Cell Proliferation. Cancer Res 2009 Mar;69(5):1867–1876.[cited 2012 Oct 11]

85. Guigon CJ, Cheng S. Novel Nongenomic Signaling of Thyroid Hormone Receptors in Thyroid Carcinogenesis. Mol Cell Endocrinol 2009 Sep;308(1-2):63–69.

86. Korkaya H, Paulson A, Iovino F, Wicha MS. HER2 regulates the mammary stem/progenitor cell population driving tumorigenesis and invasion. Oncogene 2008 Oct;27(47):6120–6130.[cited 2012 Oct 5]

87. Kroll TG, Sarraf P, Pecciarini L, Chen C-J, Mueller E, Spiegelman BM, Fletcher JA. PAX8-PPARγ1 Fusion in Oncogene Human Thyroid Carcinoma. Science 2000 Aug;289(5483):1357–1360.[cited 2012 Jun 30]

88. Powell JG, Wang X, Allard BL, Sahin M, Wang X-L, Hay ID, Hiddinga HJ, Deshpande SS, Kroll TG, Grebe SK, Eberhardt NL, McIver B. The PAX8/PPARγ

fusion oncoprotein transforms immortalized human thyrocytes through a mechanism probably involving wild-type PPARγ inhibition. Oncogene 2004;23(20):3634–3641. [cited 2012 Jun 30]

89. Au AYM, McBride C, Wilhelm KG, Koenig RJ, Speller B, Cheung L, Messina M, Wentworth J, Tasevski V, Learoyd D, Robinson BG, Clifton-Bligh RJ. PAX8-Peroxisome Proliferator-Activated Receptor γ (PPARγ) Disrupts Normal PAX8 or PPARγ Transcriptional Function and Stimulates Follicular Thyroid Cell Growth. Endocrinology 2006 Jan;147(1):367–376.[cited 2012 Jul 1]

90. Li X, Wang Z, Liu J, Tang C, Duan C, Li C. Proteomic analysis of differentially expressed proteins in normal human thyroid cells transfected with PPFP. Endocr. Relat. Cancer 2012 Oct;19(5):681–694.

91. Macchia PE, Lapi P, Krude H, Pirro MT, Missero C, Chiovato L, Souabni A, Baserga M, Tassi V, Pinchera A, Fenzi G, Grüters A, Busslinger M, Di Lauro R. PAX8 mutations associated with congenital hypothyroidism caused by thyroid dysgenesis. Nat. Genet. 1998 May;19(1):83–86.[cited 2012 Jul 5]

92. Mansouri A, Chowdhury K, Gruss P. Follicular cells of the thyroid gland require Pax8 gene function. Nat. Genet. 1998 May;19(1):87–90.[cited 2012 Jul 5]

93. Fabbro D, Pellizzari L, Mercuri F, Tell G, Damante G. Pax-8 protein levels regulate thyroglobulin gene expression. J Mol Endocrinol 1998 Dec;21(3):347–354.[cited 2012 Jul 5]

94. Ohno M, Zannini M, Levy O, Carrasco N, Lauro R di. The Paired-Domain Transcription Factor Pax8 Binds to the Upstream Enhancer of the Rat Sodium/Iodide Symporter Gene and Participates in Both Thyroid-Specific and Cyclic-AMP-Dependent Transcription. Mol. Cell. Biol. 1999 Mar;19(3):2051–2060. [cited 2012 Jul 5]

95. Esposito C, Miccadei S, Saiardi A, Civitareale D. PAX 8 activates the enhancer of the human thyroperoxidase gene. Biochemical Journal 1998 Apr;331(Pt 1):37.[cited 2012 Jul 5]

96. Magliano MP di, Lauro RD, Zannini M. Pax8 has a key role in thyroid cell differentiation. PNAS 2000 Nov;97(24):13144–13149.[cited 2012 Jul 5]

97. Tontonoz P, Spiegelman BM. Fat and Beyond: The Diverse Biology of PPARγ. Annu. Rev. Biochem. 2008 Jul;77(1):289–312.[cited 2010 Nov 5]

98. Lui W-O, Zeng L, Rehrmann V, Deshpande S, Tretiakova M, Kaplan EL, Leibiger I, Leibiger B, Enberg U, Höög A, Larsson C, Kroll TG. CREB3L2-PPARγ Fusion Mutation Identifies a Thyroid Signaling Pathway Regulated by Intramembrane Proteolysis. Cancer Research 2008;68(17):7156 –7164.[cited 2011 Aug 27]

99. Yin Y, Yuan H, Zeng X, Kopelovich L, Glazer RI. Inhibition of Peroxisome Proliferator-Activated Receptor γ Increases Estrogen Receptor–Dependent Tumor Specification. Cancer Res 2009 Jan;69(2):687–694.[cited 2012 Jul 1]

100. Yin Y, Yuan H, Wang C, Pattabiraman N, Rao M, Pestell RG, Glazer RI. 3-Phosphoinositide-Dependent Protein Kinase-1 Activates the Peroxisome Proliferator-Activated Receptor-{gamma} and Promotes Adipocyte Differentiation. Mol Endocrinol 2006 Feb;20(2):268–278.[cited 2011 Mar 30]

101. Aldred MA, Morrison C, Gimm O, Hoang-Vu C, Krause U, Dralle H, Jhiang S, Eng C. Peroxisome proliferator-activated receptor gamma is frequently downregulated in a diversity of sporadic nonmedullary thyroid carcinomas. Oncogene 2003;22(22):3412–3416.[cited 2012 Jun 30]

102. Marques AR, Espadinha C, Frias MJ, Roque L, Catarino AL, Sobrinho LG, Leite V. Underexpression of peroxisome proliferator-activated receptor (PPAR)γ in PAX8/PPARγ-negative thyroid tumours. British Journal of Cancer 2004;91(4):732–738.[cited 2012 Jun 30]

103. Park J-W, Zarnegar R, Kanauchi H, Wong MG, Hyun WC, Ginzinger DG, Lobo M, Cotter P, Duh Q-Y, Clark OH. Troglitazone, the Peroxisome Proliferator-Activated Receptor-γ Agonist, Induces Antiproliferation and Redifferentiation in Human Thyroid Cancer Cell Lines. Thyroid 2005 Mar;15(3):222–231.[cited 2012 Jun 30]

104. Kato Y, Ying H, Zhao L, Furuya F, Araki O, Willingham MC, Cheng S-Y. PPARgamma insufficiency promotes follicular thyroid carcinogenesis via activation of the nuclear factor-kappaB signaling pathway. Oncogene 2006 May;25(19):2736–2747.

105. Lacroix L, Lazar V, Michiels S, Ripoche H, Dessen P, Talbot M, Caillou B, Levillain J-P, Schlumberger M, Bidart J-M. Follicular Thyroid Tumors with the PAX8-PPARγ1 Rearrangement Display Characteristic Genetic Alterations. The American Journal of Pathology 2005 Jul;167(1):223.[cited 2012 Jun 30]

106. Fusco A, Berlingieri MT, Di Fiore PP, Portella G, Grieco M, Vecchio G. One- and two-step transformations of rat thyroid epithelial cells by retroviral oncogenes. Mol. Cell. Biol. 1987 Sep;7(9):3365–3370.

107. Matsuda T, Cepko CL. Electroporation and RNA interference in the rodent retina in vivo and in vitro. Proc. Natl. Acad. Sci. U.S.A. 2004 Jan;101(1):16–22.

108. Glass CK, Franco R, Weinberger C, Albert VR, Evans RM, Rosenfeld MG. A c-erb-A binding site in rat growth hormone gene mediates trans-activation by thyroid hormone. Nature 1987 Oct;329(6141):738–741.

109. Choi JH, Banks AS, Kamenecka TM, Busby SA, Chalmers MJ, Kumar N, Kuruvilla

DS, Shin Y, He Y, Bruning JB, Marciano DP, Cameron MD, Laznik D, Jurczak MJ, Schürer SC, Vidović D, Shulman GI, Spiegelman BM, Griffin PR. Antidiabetic actions of a non-agonist PPARγ ligand blocking Cdk5-mediated phosphorylation. Nature 2011 Sep;477(7365):477–481.[cited 2012 Jul 4]

110. Umesono K, Evans RM. Determinants of target gene specificity for steroid/thyroid hormone receptors. Cell 1989 Jun;57(7):1139–1146.

111. Lamb J, Crawford ED, Peck D, Modell JW, Blat IC, Wrobel MJ, Lerner J, Brunet J-P, Subramanian A, Ross KN, Reich M, Hieronymus H, Wei G, Armstrong SA, Haggarty SJ, Clemons PA, Wei R, Carr SA, Lander ES, Golub TR. The Connectivity Map: using gene-expression signatures to connect small molecules, genes, and disease. Science 2006 Sep;313(5795):1929–1935.

112. Lin C-L, Cheng H, Tung C-W, Huang W-J, Chang P-J, Yang J-T, Wang J-Y. Simvastatin reverses high glucose-induced apoptosis of mesangial cells via modulation of Wnt signaling pathway. Am. J. Nephrol. 2008;28(2):290–297.

113. Qiao LJ, Kang KL, Heo JS. Simvastatin promotes osteogenic differentiation of mouse embryonic stem cells via canonical Wnt/β-catenin signaling. Mol. Cells 2011 Nov;32(5):437–444.

114. Shim JS, Kim DH, Kwon HJ. Plakoglobin is a new target gene of histone deacetylase in human fibrosarcoma HT1080 cells. Oncogene 2004;23(9):1704–1711.[cited 2012 Nov 7]

115. Shang D, Liu Y, Xu X, Han T, Tian Y. 5-aza-2'-deoxycytidine enhances susceptibility of renal cell carcinoma to paclitaxel by decreasing LEF1/phospho-β-catenin expression. Cancer Lett. 2011 Dec;311(2):230–236.

116. Klinghoffer RA, Frazier J, Annis J, Berndt JD, Roberts BS, Arthur WT, Lacson R, Zhang XD, Ferrer M, Moon RT, Cleary MA. A lentivirus-mediated genetic screen identifies dihydrofolate reductase (DHFR) as a modulator of beta-catenin/GSK3 signaling. PLoS ONE 2009;4(9):e6892.

117. Georgiou KR, King TJ, Scherer MA, Zhou H, Foster BK, Xian CJ. Attenuated Wnt/β-catenin signalling mediates methotrexate chemotherapy-induced bone loss and marrow adiposity in rats. Bone 2012 Jun;50(6):1223–1233.

118. Qiu W, Chen L, Kassem M. Activation of non-canonical Wnt/JNK pathway by Wnt3a is associated with differentiation fate determination of human bone marrow stromal (mesenchymal) stem cells. Biochem. Biophys. Res. Commun. 2011 Sep;413(1):98–104.

119. Serafino A, Moroni N, Psaila R, Zonfrillo M, Andreola F, Wannenes F, Mercuri L, Rasi G, Pierimarchi P. Anti-proliferative effect of atrial natriuretic peptide on

colorectal cancer cells: evidence for an Akt-mediated cross-talk between NHE-1 activity and Wnt/β-catenin signaling. Biochim. Biophys. Acta 2012 Jun;1822(6):1004–1018.

120. Doshi LS, Brahma MK, Bahirat UA, Dixit AV, Nemmani KVS. Discovery and development of selective PPAR gamma modulators as safe and effective antidiabetic agents. Expert Opin Investig Drugs 2010 Apr;19(4):489–512.

121. Östberg T, Svensson S, Selén G, Uppenberg J, Thor M, Sundbom M, Sydow-Bäckman M, Gustavsson A-L, Jendeberg L. A New Class of Peroxisome Proliferator-activated Receptor Agonists with a Novel Binding Epitope Shows Antidiabetic Effects. J. Biol. Chem. 2004 Sep;279(39):41124–41130.[cited 2012 Nov 12]

122. Rocchi S, Picard F, Vamecq J, Gelman L, Potier N, Zeyer D, Dubuquoy L, Bac P, Champy M-F, Plunket KD, Leesnitzer LM, Blanchard SG, Desreumaux P, Moras D, Renaud J-P, Auwerx J. A Unique PPAR[gamma] Ligand with Potent Insulin-Sensitizing yet Weak Adipogenic Activity. Molecular Cell 2001 Oct;8(4):737–747. [cited 2011 Jan 12]

123. Choi JH, Banks AS, Estall JL, Kajimura S, Bostrom P, Ruas JL, Chalmers MJ, Kamenecka TM, Bluher M, Griffin PR, Spiegelman BM. Anti-diabetic drugs inhibit obesity-linked phosphorylation of PPAR[ggr] by Cdk5. Nature 2010 Jul;466(7305):451–456.[cited 2010 Nov 5]

124. Diallo-Krou E, Yu J, Colby LA, Inoki K, Wilkinson JE, Thomas DG, Giordano TJ, Koenig RJ. Paired Box Gene 8-Peroxisome Proliferator-Activated Receptor-γ Fusion Protein and Loss of Phosphatase and Tensin Homolog Synergistically Cause Thyroid Hyperplasia in Transgenic Mice. Endocrinology 2009 Nov;150(11):5181–5190.[cited 2012 Jul 1]

125. Reddi HV, Madde P, Milosevic D, Hackbarth JS, Algeciras-Schimnich A, McIver B, Grebe SKG, Eberhardt NL. The Putative PAX8/PPARγ Fusion Oncoprotein Exhibits Partial Tumor Suppressor Activity through Up-Regulation of Micro-RNA-122 and Dominant-Negative PPARγ Activity. Genes & Cancer 2011 Jan;2(1):46–55.[cited 2012 Jul 1]

126. Espadinha C, Cavaco BM, Leite V. PAX8PPARgamma stimulates cell viability and modulates expression of thyroid-specific genes in a human thyroid cell line. Thyroid 2007 Jun;17(6):497–509.[cited 2010 Dec 13]

127. Zhang J, Gill AJM, Issacs JD, Atmore B, Johns A, Delbridge LW, Lai R, McMullen TPW. The Wnt/β-catenin pathway drives increased cyclin D1 levels in lymph node metastasis in papillary thyroid cancer. Hum. Pathol. 2012 Jul;43(7):1044–1050. [cited 2012 Jul 2]

128. Wood WM, Sharma V, Bauerle KT, Pike LA, Zhou Q, Fretwell DL, Schweppe RE, Haugen BR. PPARγ Promotes Growth and Invasion of Thyroid Cancer Cells. PPAR Res 2011;2011:171765.

129. Kastan MB, Schlaffer E, Russo JE, Colvin OM, Civin CI, Hilton J. Direct demonstration of elevated aldehyde dehydrogenase in human hematopoietic progenitor cells. Blood 1990 May;75(10):1947–1950.

130. Goretzki PE, Frilling A, Simon D, Roeher HD. Growth regulation of normal thyroids and thyroid tumors in man. Recent Results Cancer Res. 1990;118:48–63.

131. Dontu G, Abdallah WM, Foley JM, Jackson KW, Clarke MF, Kawamura MJ, Wicha MS. In vitro propagation and transcriptional profiling of human mammary stem/progenitor cells. Genes Dev. 2003 May;17(10):1253–1270.[cited 2012 Dec 4]

132. Cross DA, Alessi DR, Cohen P, Andjelkovich M, Hemmings BA. Inhibition of glycogen synthase kinase-3 by insulin mediated by protein kinase B. Nature 1995 Dec;378(6559):785–789.

133. Rao AS, Kremenevskaja N, Resch J, Brabant G. Lithium stimulates proliferation in cultured thyrocytes by activating Wnt/beta-catenin signalling. Eur. J. Endocrinol. 2005 Dec;153(6):929–938.[cited 2012 Jul 2]

134. Kim WB, Lewis CJ, McCall KD, Malgor R, Kohn AD, Moon RT, Kohn LD. Overexpression of Wnt-1 in thyrocytes enhances cellular growth but suppresses transcription of the thyroperoxidase gene via different signaling mechanisms. Journal of Endocrinology 2007 Apr;193(1):93 –106.[cited 2011 Aug 27]

135. Chen G, Jiang Q, You Z, Yao J, Mou L, Lin X, Shen X, You T, Lin Q, Wen J, Lin L. Regulation of GSK-3 beta in the proliferation and apoptosis of human thyrocytes investigated using a GSK-3 beta-targeting RNAi adenovirus expression vector: involvement the Wnt/beta-catenin pathway. Mol. Biol. Rep 2010 Jul;37(6):2773–2779.[cited 2011 Aug 27]

136. Rocheleau CE, Downs WD, Lin R, Wittmann C, Bei Y, Cha YH, Ali M, Priess JR, Mello CC. Wnt signaling and an APC-related gene specify endoderm in early C. elegans embryos. Cell 1997 Aug;90(4):707–716.

137. Thorpe CJ, Schlesinger A, Carter JC, Bowerman B. Wnt signaling polarizes an early C. elegans blastomere to distinguish endoderm from mesoderm. Cell 1997 Aug;90(4):695–705.

138. Gregorieff A, Clevers H. Wnt signaling in the intestinal epithelium: from endoderm to cancer. Genes Dev. 2005 Apr;19(8):877–890.

139. Gilbert-Sirieix M, Makoukji J, Kimura S, Talbot M, Caillou B, Massaad C,

Massaad-Massade L. Wnt/β-catenin signaling pathway is a direct enhancer of thyroid transcription factor-1 in human papillary thyroid carcinoma cells. PLoS ONE 2011;6(7):e22280.

140. Burgermeister E, Schnoebelen A, Flament A, Benz J, Stihle M, Gsell B, Rufer A, Ruf A, Kuhn B, Marki HP, Mizrahi J, Sebokova E, Niesor E, Meyer M. A Novel Partial Agonist of Peroxisome Proliferator-Activated Receptor-{gamma} (PPAR{gamma}) Recruits PPAR{gamma}-Coactivator-1{alpha}, Prevents Triglyceride Accumulation, and Potentiates Insulin Signaling in Vitro. Mol Endocrinol 2006 Apr;20(4):809–830.[cited 2010 Dec 30]

141. Gregoire FM, Zhang F, Clarke HJ, Gustafson TA, Sears DD, Favelyukis S, Lenhard J, Rentzeperis D, Clemens LE, Mu Y, Lavan BE. MBX-102/JNJ39659100, a Novel Peroxisome Proliferator-Activated Receptor-Ligand with Weak Transactivation Activity Retains Antidiabetic Properties in the Absence of Weight Gain and Edema. Mol Endocrinol 2009 Jul;23(7):975–988.[cited 2010 Nov 9]

142. Fujimura T, Sakuma H, Konishi S, Oe T, Hosogai N, Kimura C, Aramori I, Mutoh S. FK614, a novel peroxisome proliferator-activated receptor gamma modulator, induces differential transactivation through a unique ligand-specific interaction with transcriptional coactivators. J. Pharmacol. Sci 2005 Dec;99(4):342–352.[cited 2011 May 24]

143. Oberfield JL, Collins JL, Holmes CP, Goreham DM, Cooper JP, Cobb JE, Lenhard JM, Hull-Ryde EA, Mohr CP, Blanchard SG, Parks DJ, Moore LB, Lehmann JM, Plunket K, Miller AB, Milburn MV, Kliewer SA, Willson TM. A peroxisome proliferator-activated receptor γ ligand inhibits adipocyte differentiation. PNAS 1999 May;96(11):6102–6106.[cited 2012 Dec 3]

144. Fujimura T, Kimura C, Oe T, Takata Y, Sakuma H, Aramori I, Mutoh S. A Selective Peroxisome Proliferator-Activated Receptor γ Modulator with Distinct Fat Cell Regulation Properties. Journal of Pharmacology and Experimental Therapeutics 2006;318(2):863 –871.[cited 2011 May 24]

145. Wen X, Li Y, Liu Y. Opposite Action of Peroxisome Proliferator-activated Receptor-γ in Regulating Renal Inflammation. Journal of Biological Chemistry 2010;285(39):29981 –29988.[cited 2011 Sep 22]